

EIC at small- x : connections to p+p/A & A+A physics at RHIC & LHC

Prithwish Tribedy



13th Conference on the Intersections of Particle and Nuclear Physics

May 29 – June 3, 2018 Palm Springs, CA



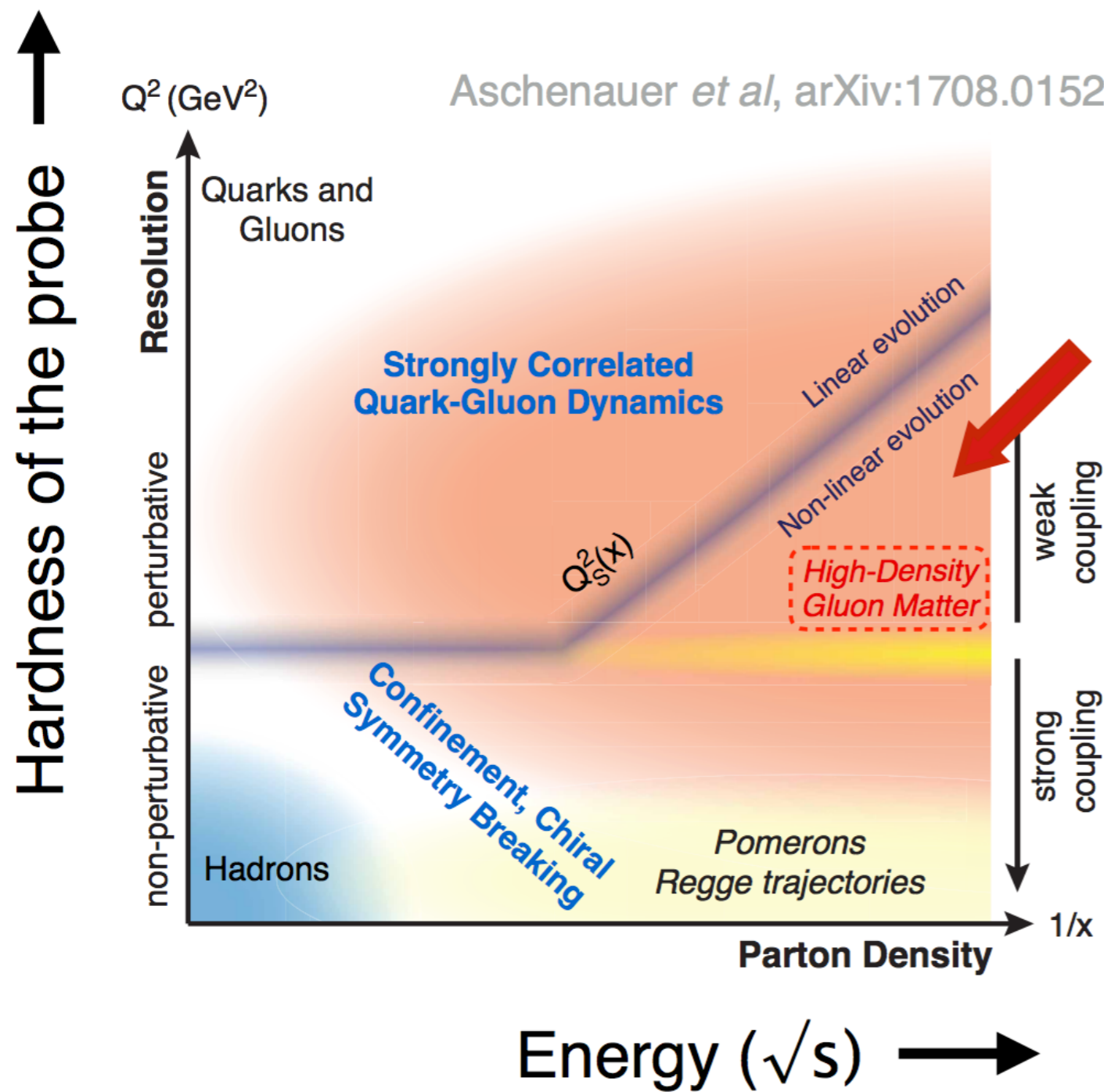
U.S. DEPARTMENT OF
ENERGY

Office of
Science

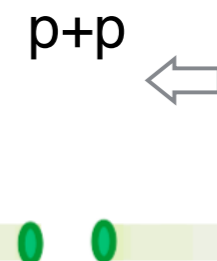
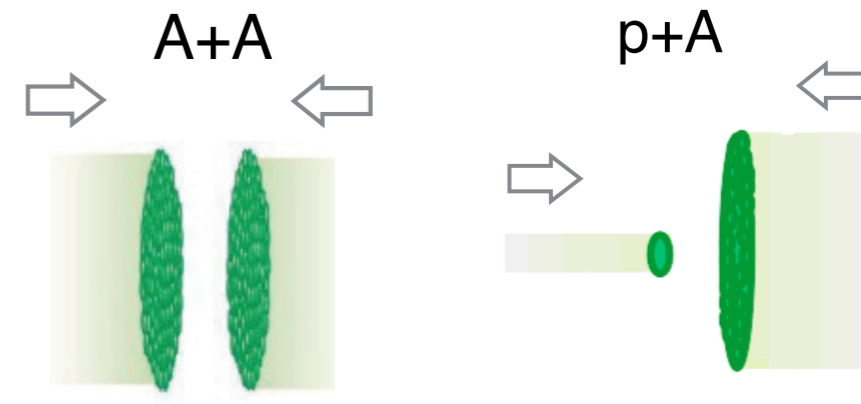
Outline

- HERA e+p data & modeling p+p/A & A+A collisions at small-x
- Correlation measurements & phenomenology at RHIC/LHC
- Towards phenomenology of EIC : can lessons from RHIC/LHC help ?

The landscape of QCD

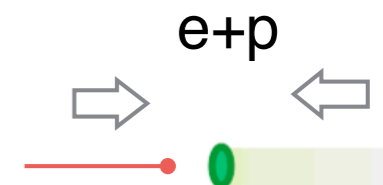
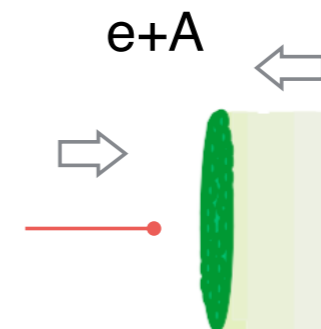


RHIC and LHC
(present days)



Future (EIC)

Past (HERA)

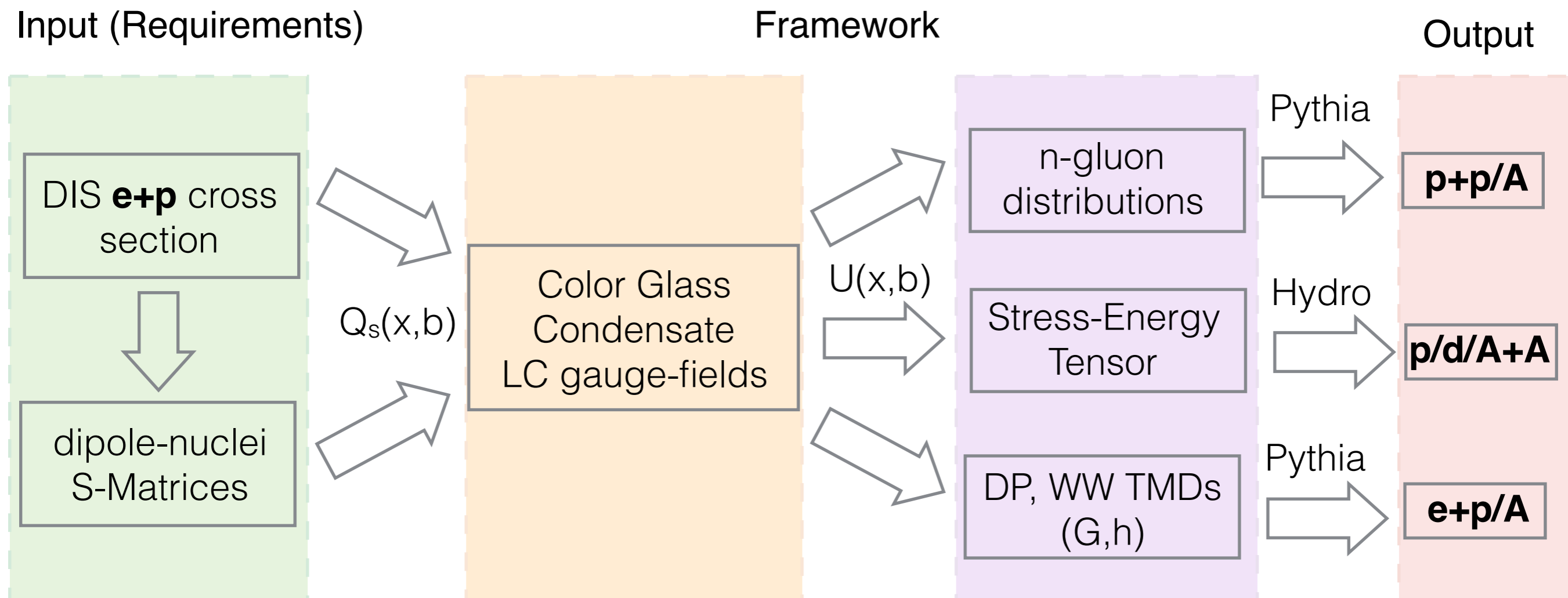


At small- $x \rightarrow$ universal framework for e+p, e+A to p+p, p+A & A+A

Universal approach at small-x

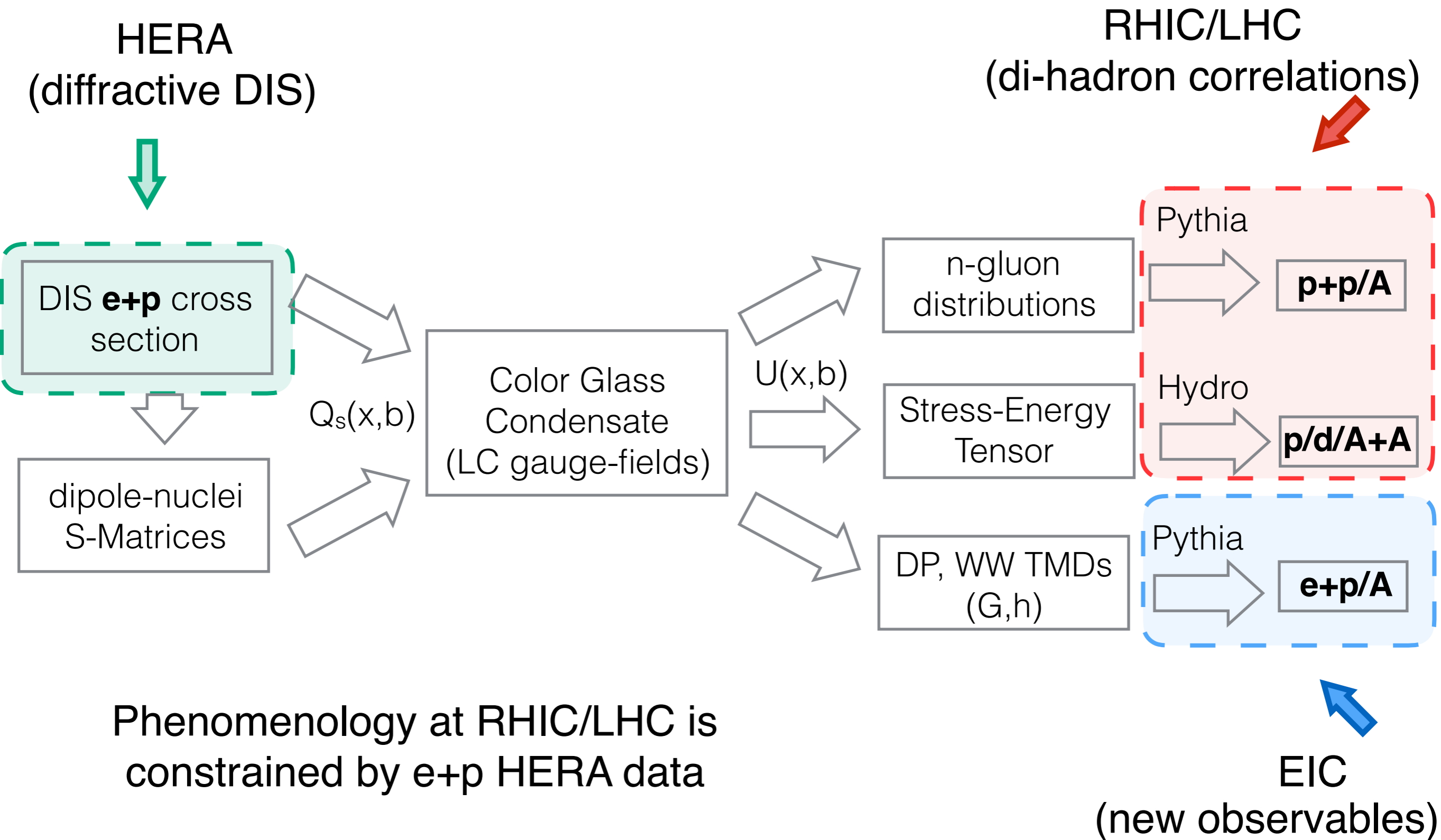
Where are the connections ?

Flow chart of phenomenology in p+p/A & A+A at high energy, small-x



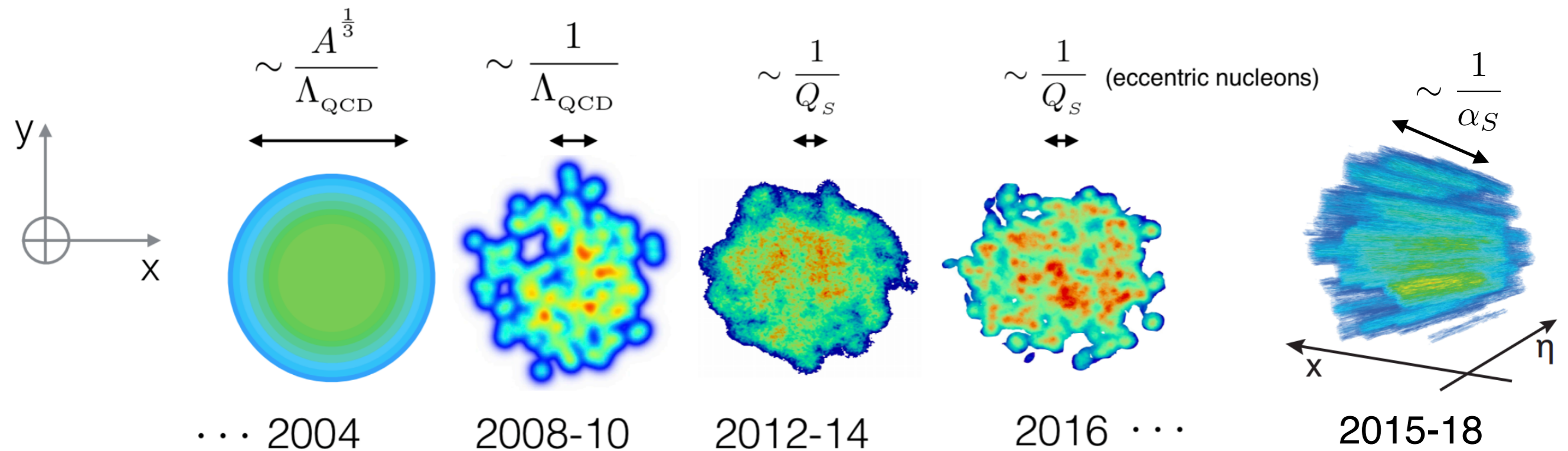
State-of-the art phenomenology at RHIC/LHC

Where are the connections ?



Heavy ion physics@RHIC/LHC: uncertainties

Biggest uncertainty : initial stages of the colliding nuclei



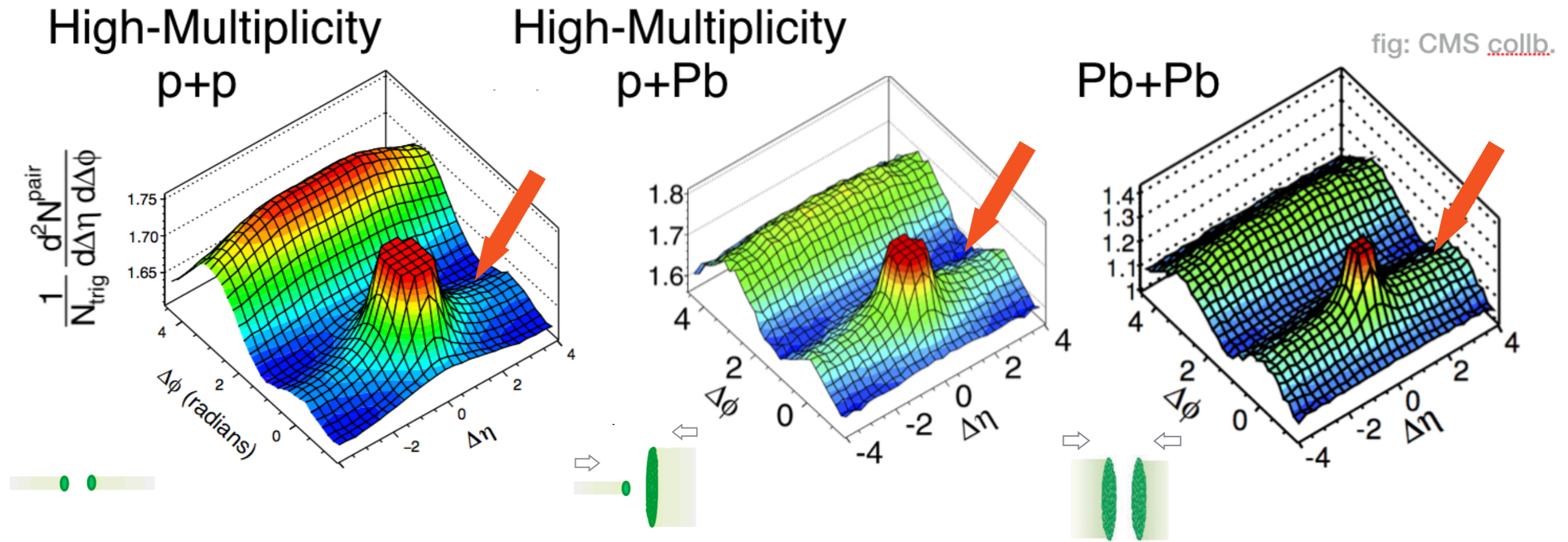
Transverse geometry : our understanding has improved over the years

Longitudinal structure : we have only started to explore

EIC → ultimate machine, how can we use the lessons from RHIC/LHC

Experimental observables in $p+p/A, A+A$

Long range azimuthal correlations : Ridge

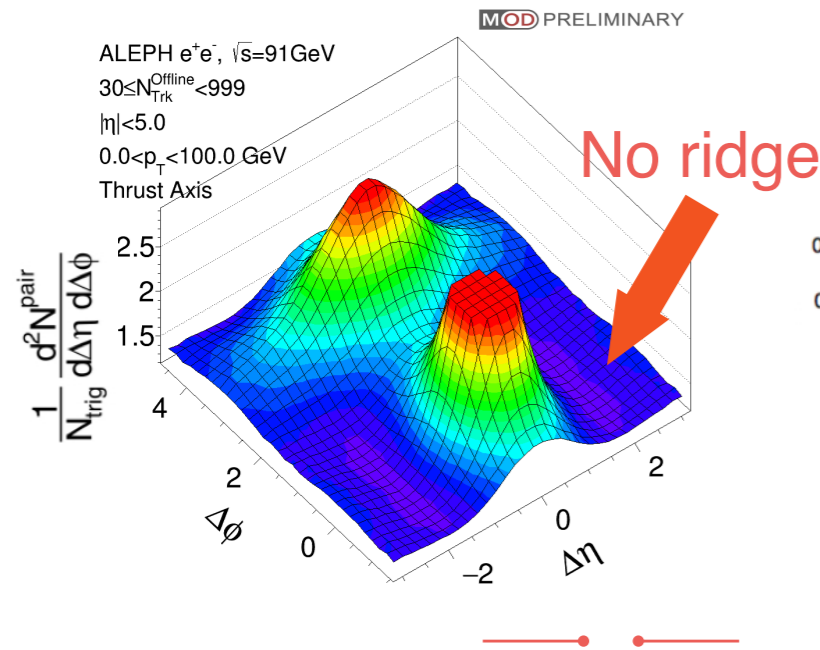


Ridge phenomenon (most striking and widely studied):
Di-hadron correlations in relative pseudorapidity ($\Delta\eta$) & azimuth ($\Delta\phi$)
High multiplicity p+p/A \rightarrow strikingly similar to A+A

Ridge across different collision systems

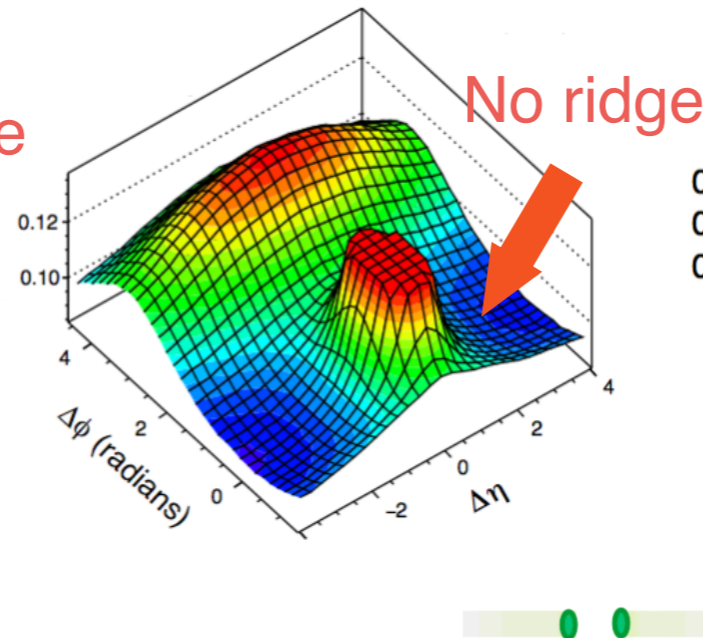
Y-J. Lee, QM'18

e⁺e⁻



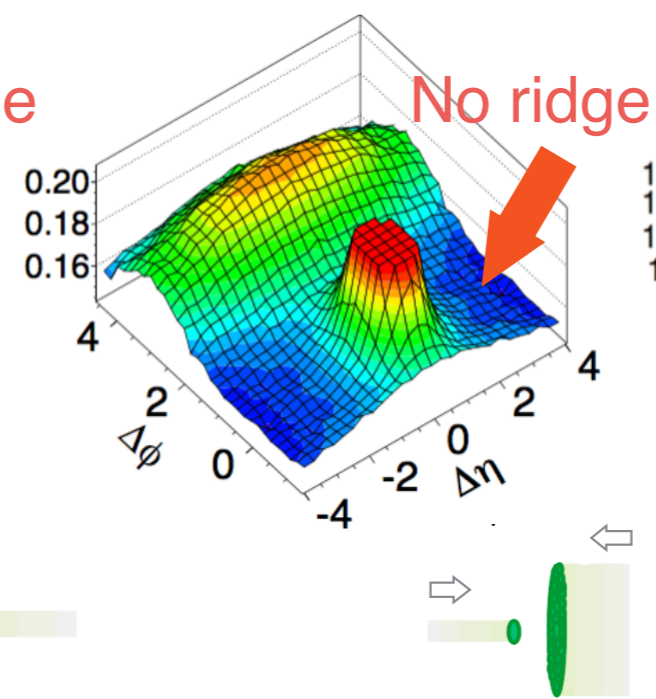
Low multiplicity

p+p



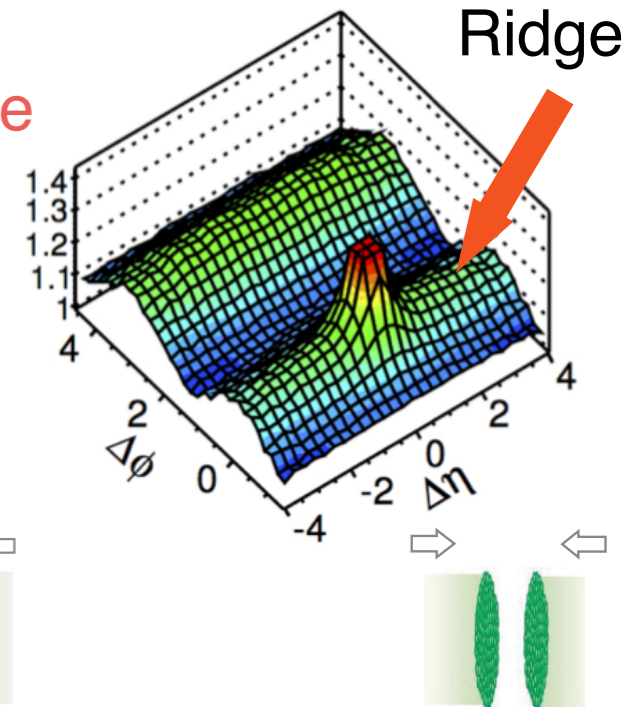
Low multiplicity

p+A



CMS collaboration

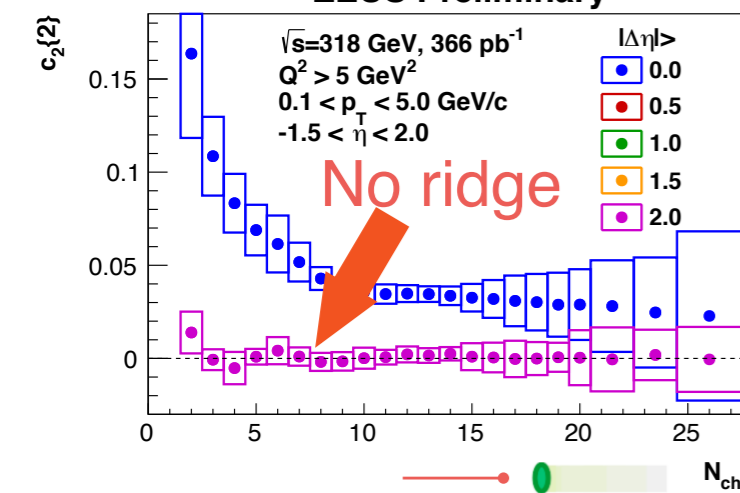
A+A



J. Onderwaater, QM'18

e+p

ZEUS Preliminary

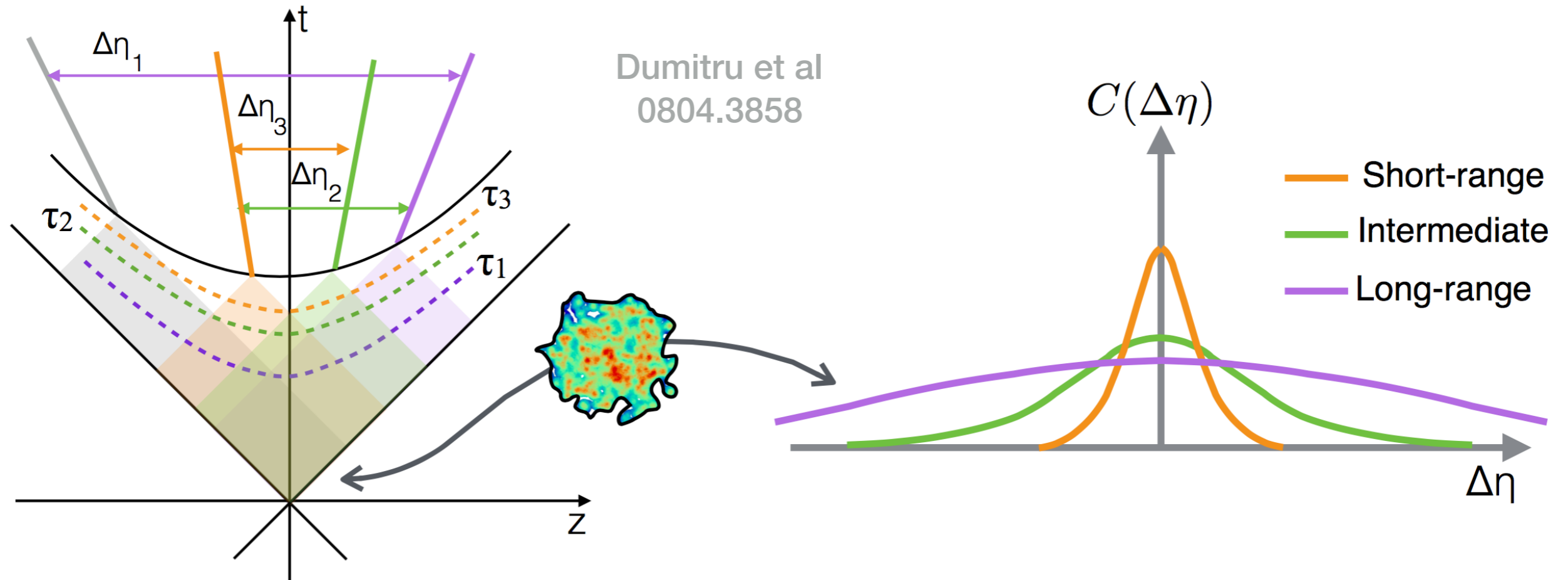


No ridge appears in e+e, e+p, and low multiplicity p+p/A collisions

Interesting systematics with collisions system

The qualitative picture : what drives ridge ?

Dynamics of early time spread over wide range of rapidity



Causality limits signals from different τ to spread at different $\Delta\eta$

Long-range rapidity correlations \rightarrow generated at early times

The qualitative picture : what drives ridge ?

Initial state correlations (colliding hadrons/nuclei)

Momentum space correlations

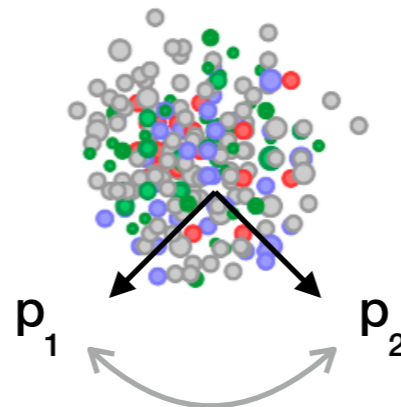
Position space correlations

(Mini-) jets,
n-parton correlations

Initial spatial anisotropy

Fragmentation

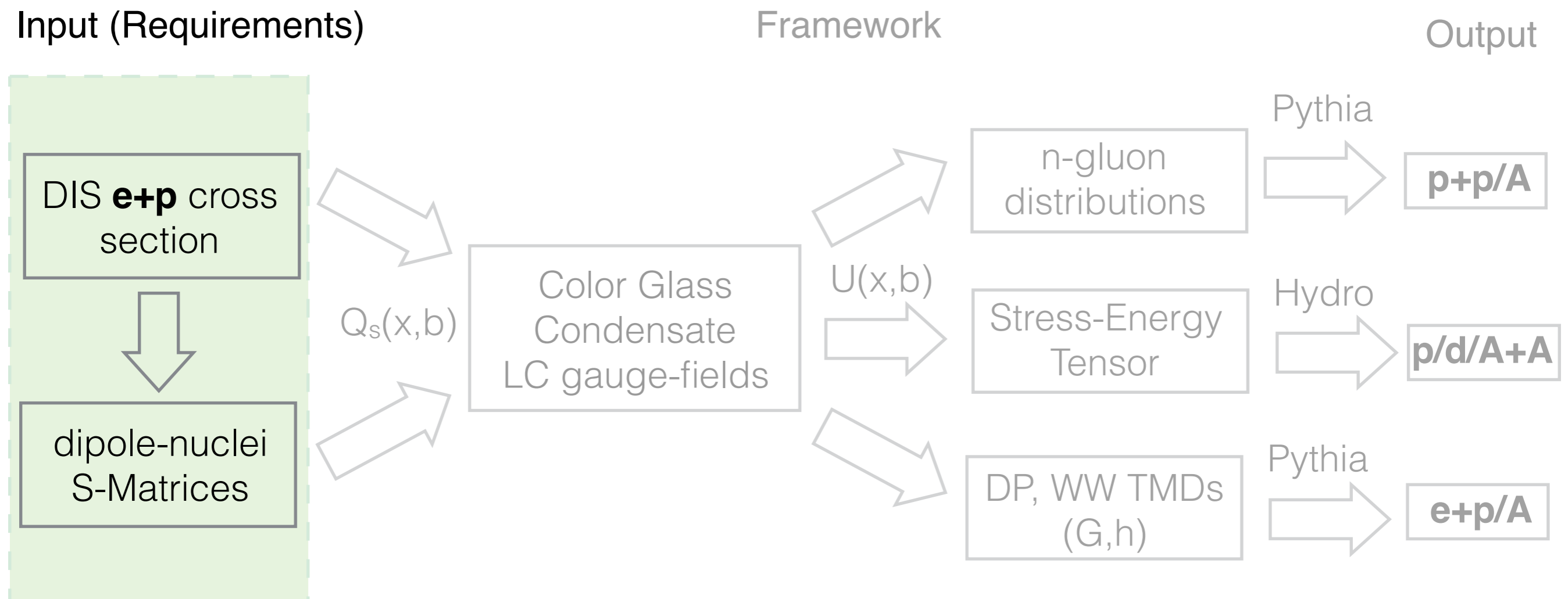
Transport,
Hydrodynamic



Experimentally observed correlations (both should contribute)

Phenomenology at small-x

Flow chart of phenomenology in p+p/A & A+A at high energy, small-x



State-of-the art phenomenology at RHIC/LHC

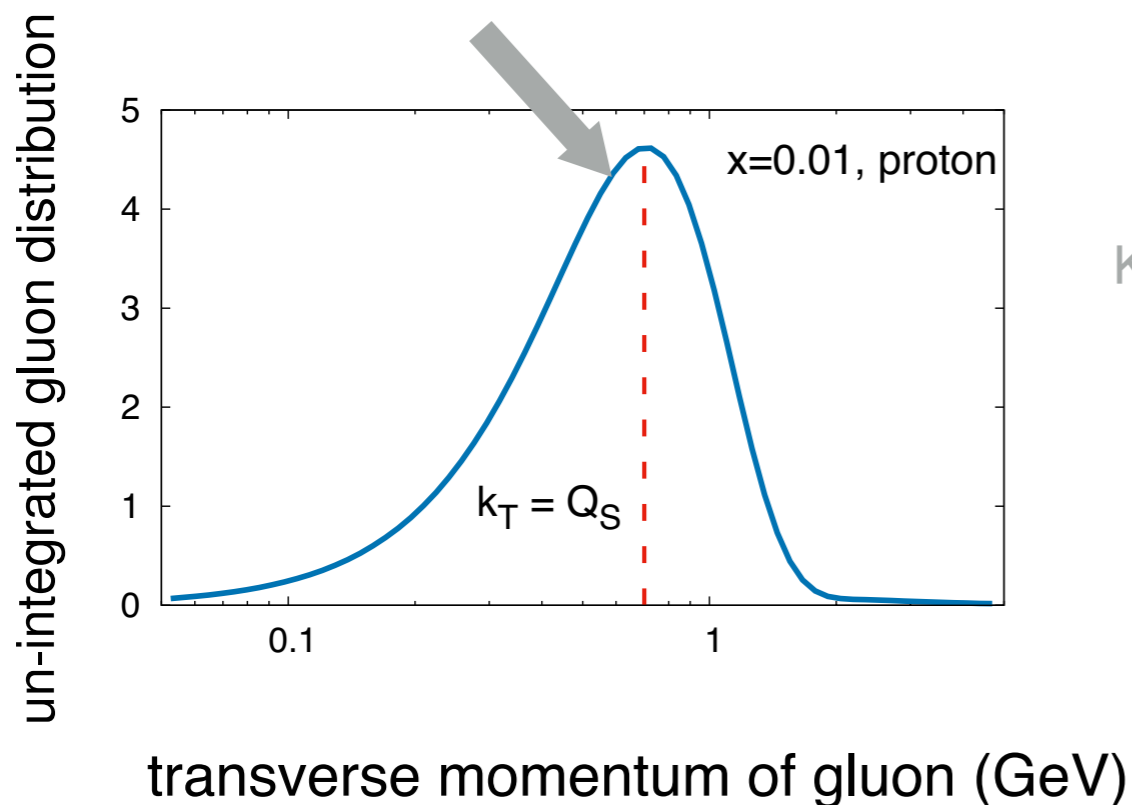
Colliding protons at small-x

Ridge \rightarrow long-range correlations \rightarrow driven by initial state effects

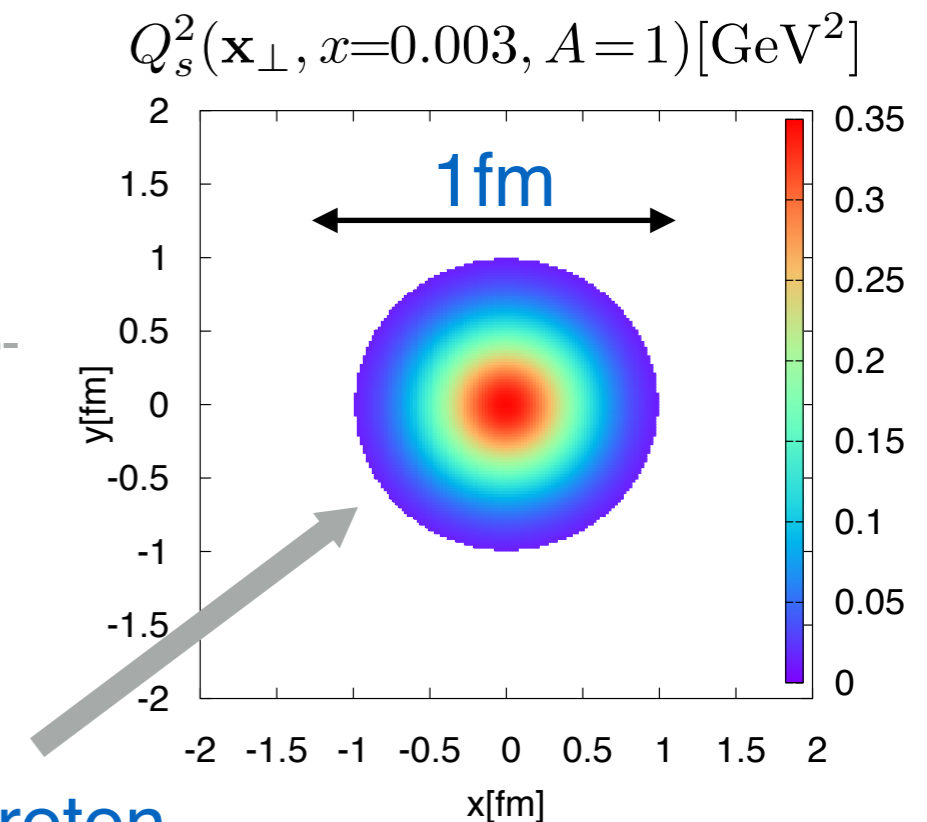
Ridge probes the wave function of colliding hadrons/nuclei

Momentum Space

Most gluons are here ($\sim Q_s$)



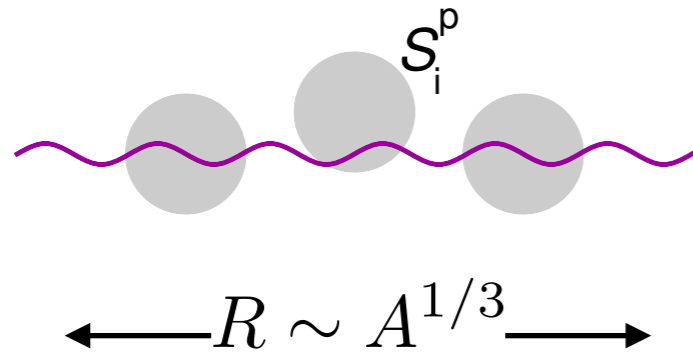
Coordinate Space



Input : HERA DIS e+p coherent diffractive cross section : $\frac{d\sigma^{\gamma^* p \rightarrow J/\Psi p}}{dt}$

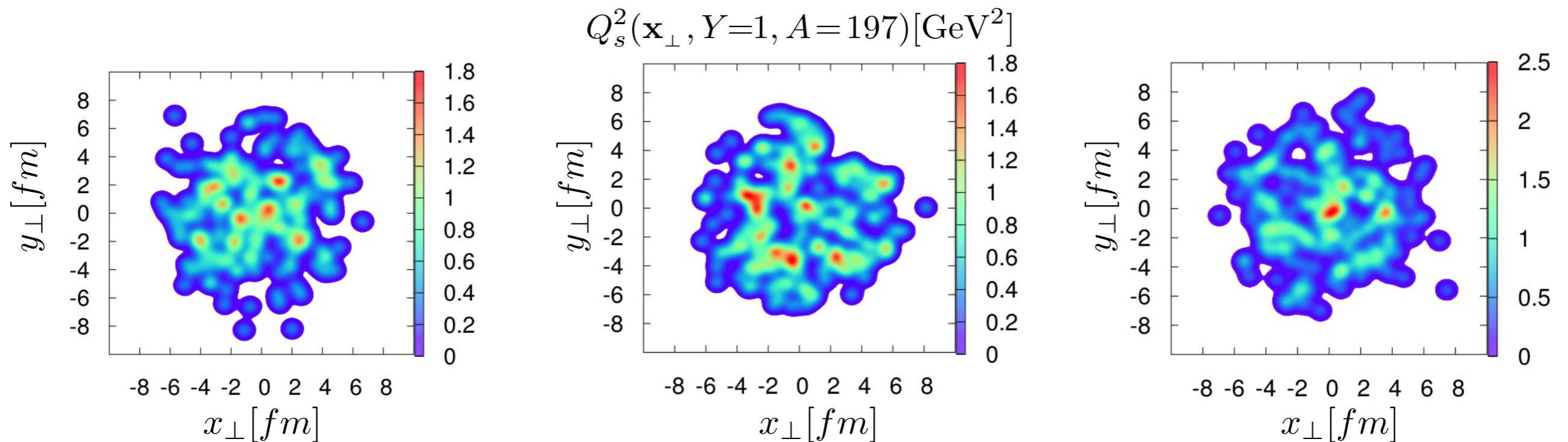
Colliding nuclei at small-x : IP-Sat/Glasma

Nucleus \rightarrow multiple scattering centers (from Glauber) + IP-Sat :



$$S_{\text{dip}}^A(\mathbf{r}_\perp, x, \mathbf{b}_\perp) = \prod_{i=0}^A S_{\text{dip}}^p(\mathbf{r}_\perp, x, \mathbf{b}_\perp)$$

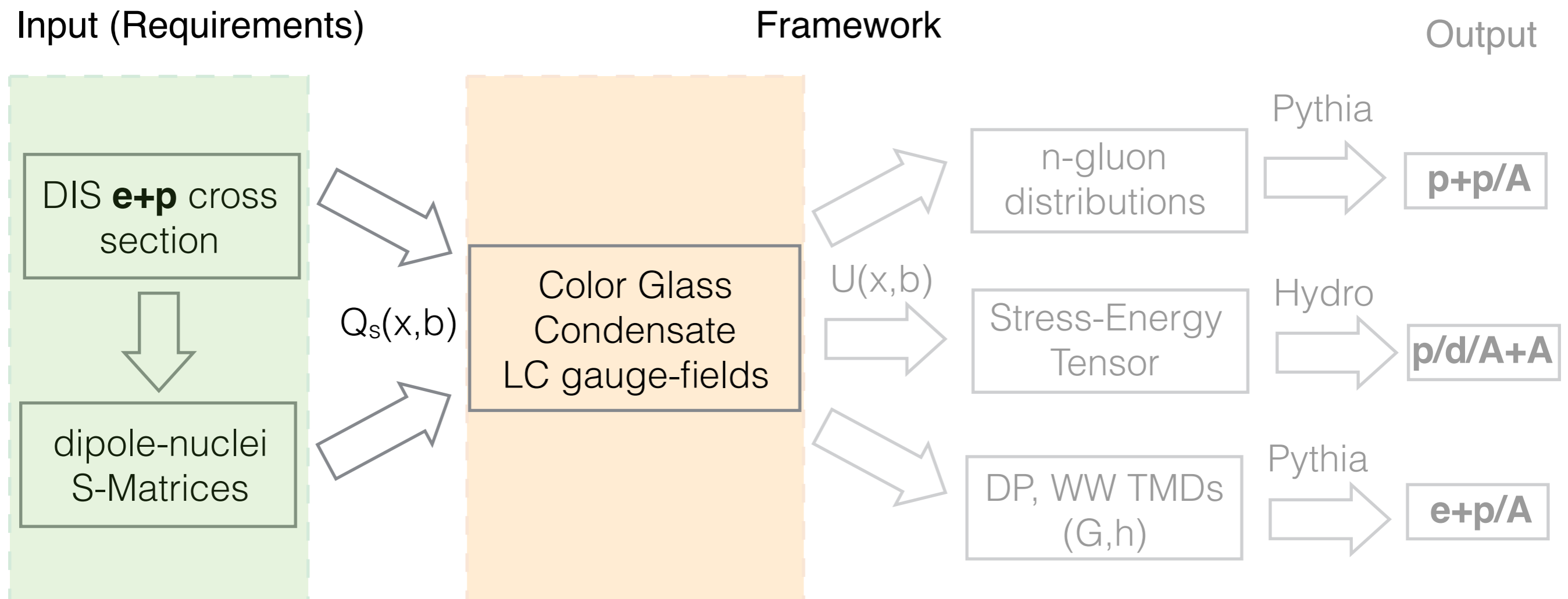
$Q_{s,A}^2(\sqrt{s}) \sim A^{1/3} Q_{s,\text{proton}}(\sqrt{s}) \rightarrow$ less boost is needed to saturate nuclei



One obtains saturation scales for different configurations of a nucleus

Phenomenology at small-x

Flow chart of phenomenology in p+p/A & A+A at high energy, small-x



State-of-the art phenomenology at RHIC/LHC

Color Glass Condensate, MV model, Glasma

Schenke, PT, Venugopalan Phys. Rev. Lett. 108 (2012) 252301

- Fundamental objects are Color Charge density matrices $\rho^a(x_\perp, Y)$, local Gaussian distribution $W[\rho]$ (MV-Model)

$$\langle \rho^a(\mathbf{x}_\perp) \rho^b(\mathbf{y}_\perp) \rangle \propto \delta^{ab} \delta^2(\mathbf{x}_\perp - \mathbf{y}_\perp) Q_s^2(\mathbf{x}_\perp)$$

- Color field before collisions : solving Yang Mills equations for each configuration of source $\rho(x_\perp)$ & current $J^\nu = \delta^\nu \rho(x_\perp)$

$$[D_\mu, F^{\mu\nu}] = J^\nu$$

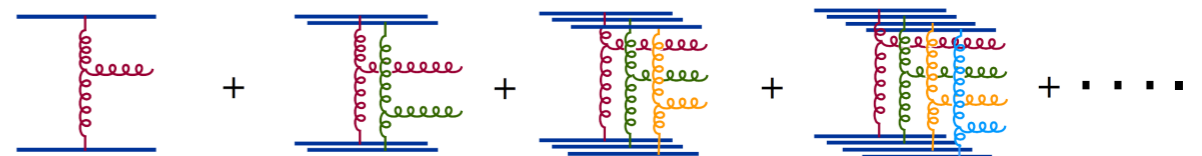
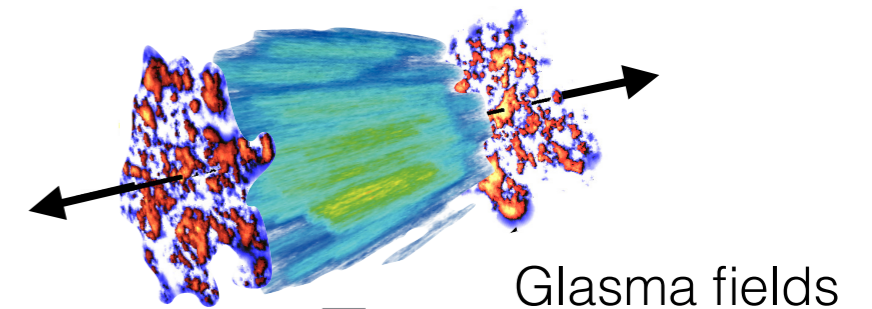
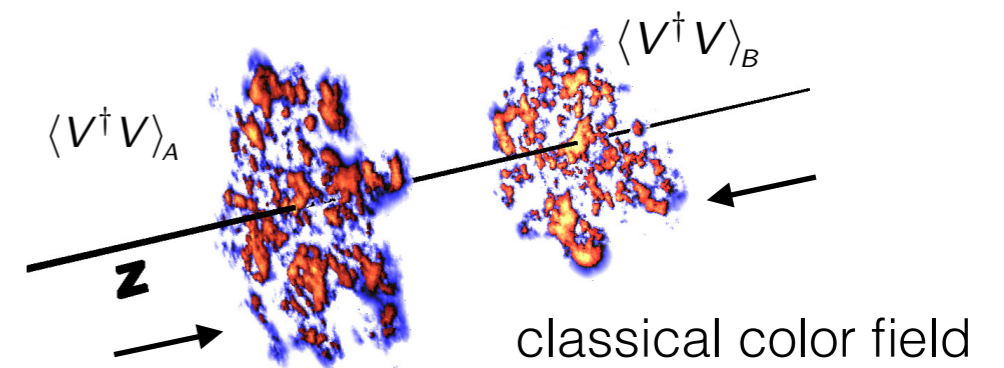
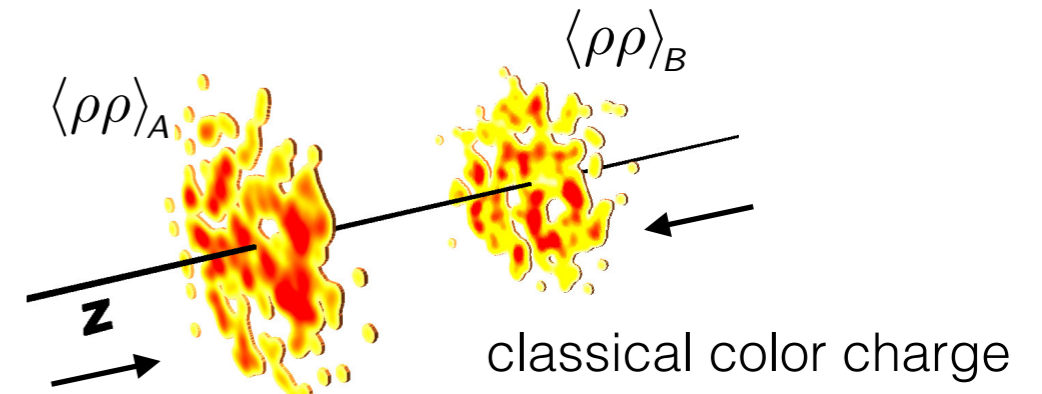
- Compute & evolve the color fields after collisions :

$$A^i = A_{(A)}^i + A_{(B)}^i \quad A^\eta = \frac{ig}{2} [A_{(A)}^i, A_{(B)}^i]$$

Light-cone gauge fields $A^i(x_\perp)$

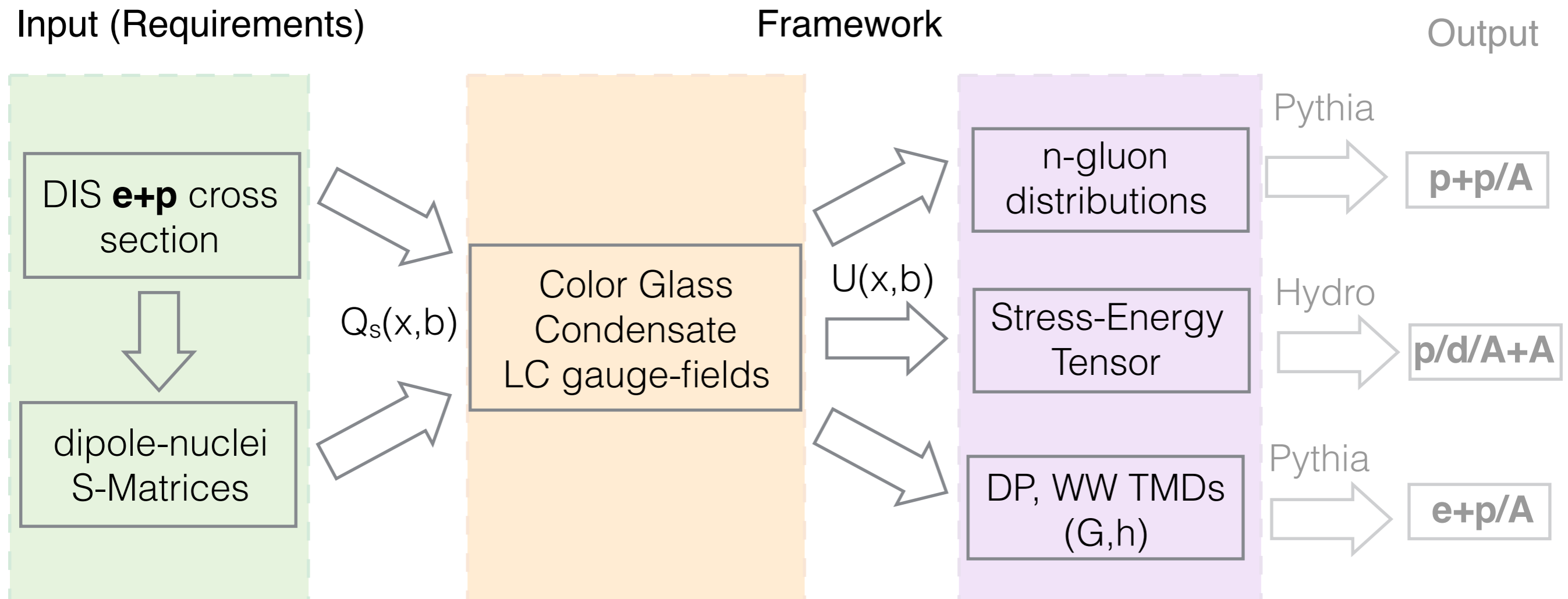
→ Building blocks for any calculation

hep-ph/9809433, hep-ph/0303076,
arXiv:1206.6805, arXiv: 1202.6646



Phenomenology at small-x

Flow chart of phenomenology in p+p/A & A+A at high energy, small-x



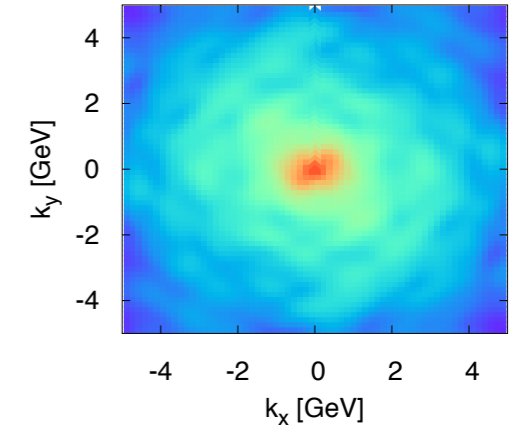
State-of-the art phenomenology at RHIC/LHC

Initial state correlations

Momentum space correlations : n-gluon distribution

$$\frac{dN_g}{dy} = \frac{2}{N^2} \int \frac{d^2 k_T}{\tilde{k}_T} \left[\frac{g^2}{\tau} \text{tr} (E_i(\mathbf{k}_\perp) E_i(-\mathbf{k}_\perp)) + \tau \text{tr} (\pi(\mathbf{k}_\perp) \pi(-\mathbf{k}_\perp)) \right]$$

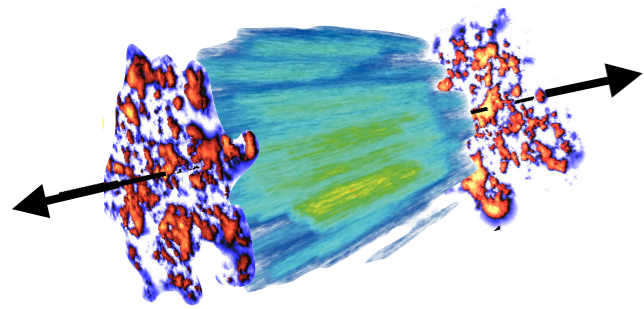
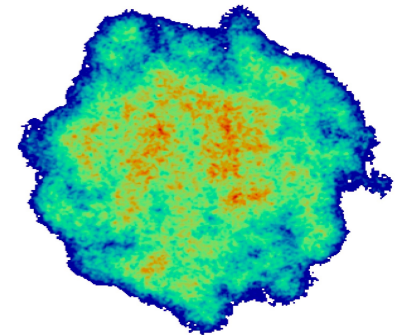
Input to PYTHIA, p+p/A collisions



Position space correlations : Stress-Energy Tensor

$$T^{\mu\nu} = -g^{\gamma\delta} F_\gamma^\mu F_\delta^\nu + \frac{1}{4} g^{\mu\nu} F_\delta^\gamma F_\gamma^\delta$$

Input to hydro, transport, p+A, A+A collisions



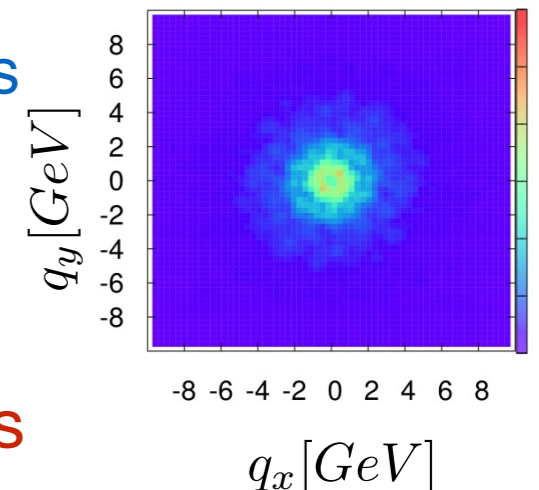
Light-cone gauge-fields

$$U(\mathbf{x}_T) = \mathbb{P} \exp \left\{ ig \int dx^- A^+(x^-, \mathbf{x}_T) \right\}$$

Wave functions: Dipole-gluon & WWs TMDs

$$xG_{\text{WW}}^{ij}(x, \vec{k}) = \frac{8\pi}{L^2} \int \frac{d^2 \mathbf{x}_T}{(2\pi)^2} \frac{d^2 \mathbf{y}_T}{(2\pi)^2} e^{-i\mathbf{k}_T \cdot (\mathbf{x}_T - \mathbf{y}_T)} \times \langle A_a^i(\mathbf{x}_T) A_a^j(\mathbf{y}_T) \rangle$$

Input for EIC observables e+p/A collisions

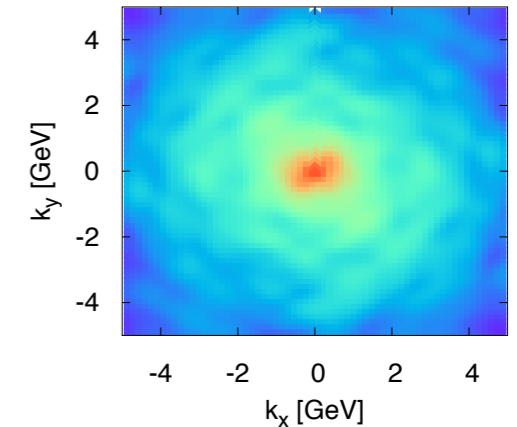


Momentum space correlations

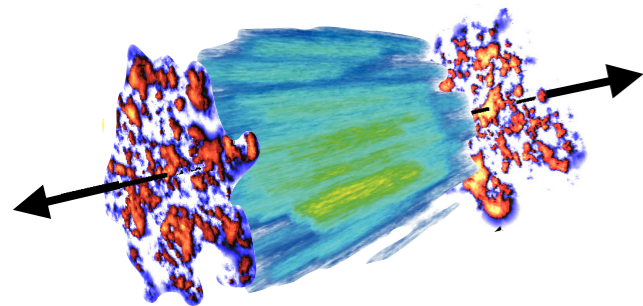
Momentum space correlations : n-gluon distribution

$$\frac{dN_g}{dy} = \frac{2}{N^2} \int \frac{d^2 k_T}{\tilde{k}_T} \left[\frac{g^2}{\tau} \text{tr} (E_i(\mathbf{k}_\perp) E_i(-\mathbf{k}_\perp)) + \tau \text{tr} (\pi(\mathbf{k}_\perp) \pi(-\mathbf{k}_\perp)) \right]$$

Input to PYTHIA, p+p/A collisions



Light-cone gauge-fields

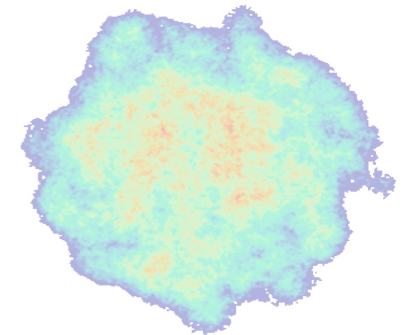


$$U(\mathbf{x}_T) = \mathbb{P} \exp \left\{ ig \int dx^- A^+(x^-, \mathbf{x}_T) \right\}$$

Position space correlations : Stress-Energy Tensor

$$T^{\mu\nu} = -g^{\gamma\delta} F_\gamma^\mu F_\delta^\nu + \frac{1}{4} g^{\mu\nu} F_\delta^\gamma F_\gamma^\delta$$

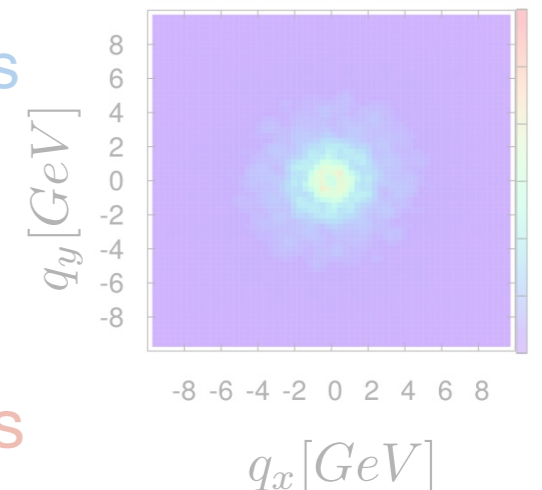
Input to hydro, transport, p+A, A+A collisions



Wave functions: Dipole-gluon & WWs TMDs

$$xG_{\text{WW}}^{ij}(x, \vec{k}) = \frac{8\pi}{L^2} \int \frac{d^2 \mathbf{x}_T}{(2\pi)^2} \frac{d^2 \mathbf{y}_T}{(2\pi)^2} e^{-i\mathbf{k}_T \cdot (\mathbf{x}_T - \mathbf{y}_T)} \times \langle A_a^i(\mathbf{x}_T) A_a^j(\mathbf{y}_T) \rangle$$

Input for EIC observables e+p/A collisions

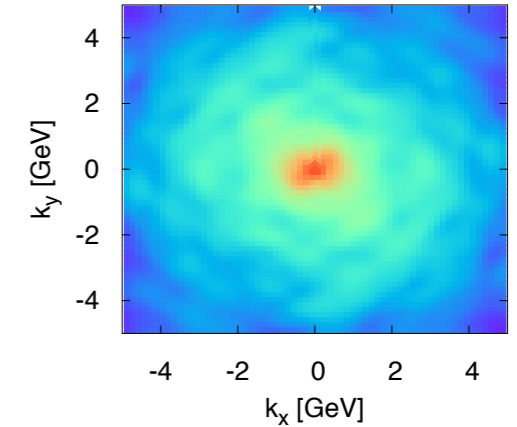


Success of small-x phenomenology in p+p/A

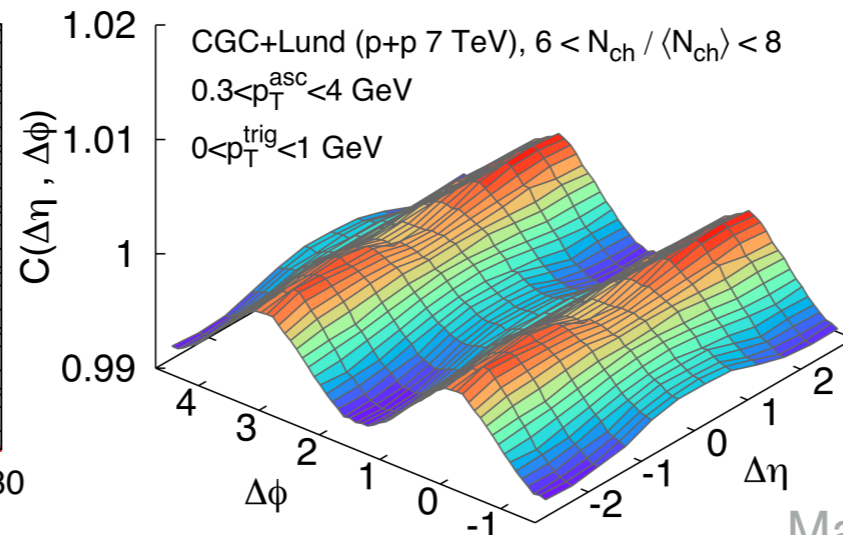
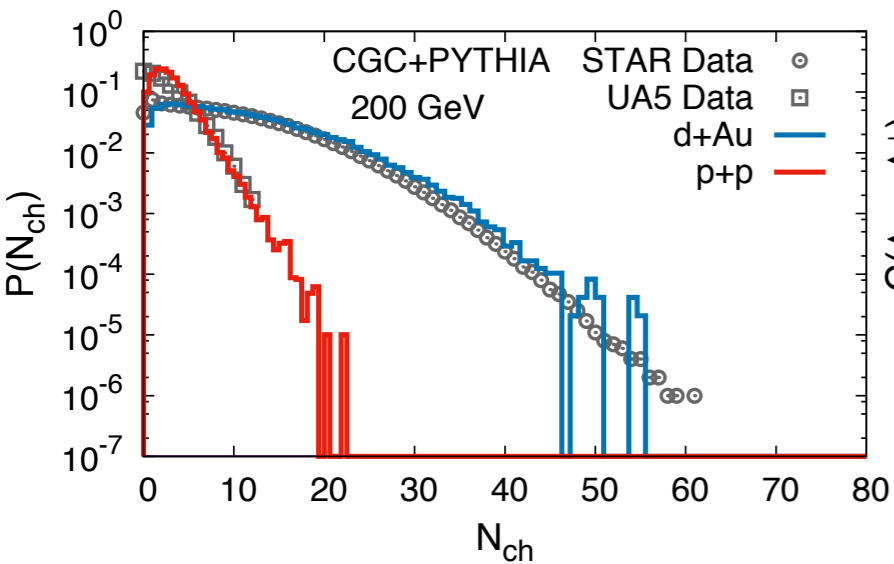
Momentum space correlations : n-gluon distribution

$$\frac{dN_g}{dy} = \frac{2}{N^2} \int \frac{d^2 k_T}{\tilde{k}_T} \left[\frac{g^2}{\tau} \text{tr} (E_i(\mathbf{k}_\perp) E_i(-\mathbf{k}_\perp)) + \tau \text{tr} (\pi(\mathbf{k}_\perp) \pi(-\mathbf{k}_\perp)) \right]$$

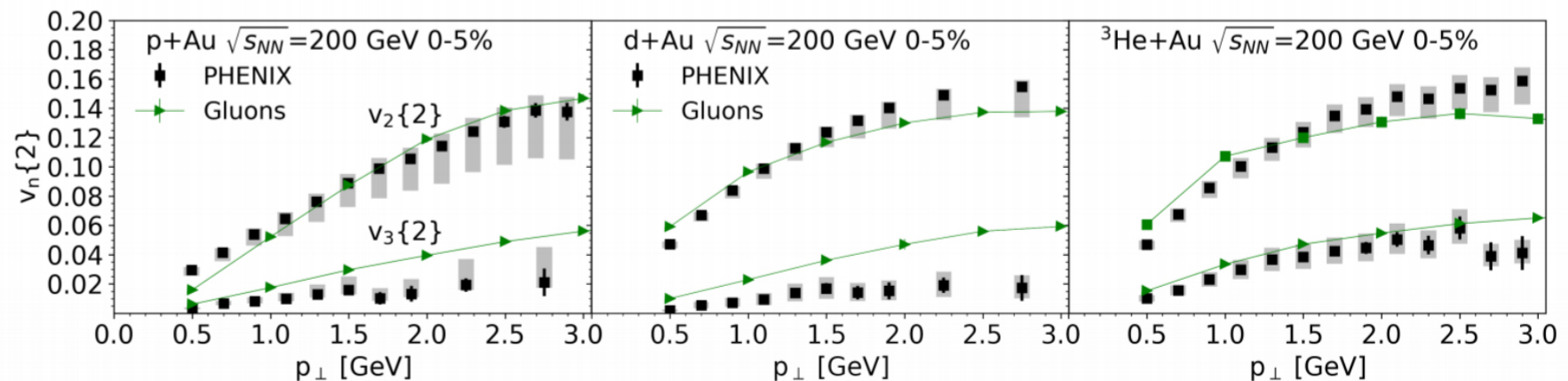
Input to PYTHIA, p+p/A collisions



Schenke, Schlichting, PT, Venugopalan 1607.02496



Mace, Skokov, PT, Venugopalan 1805.09342

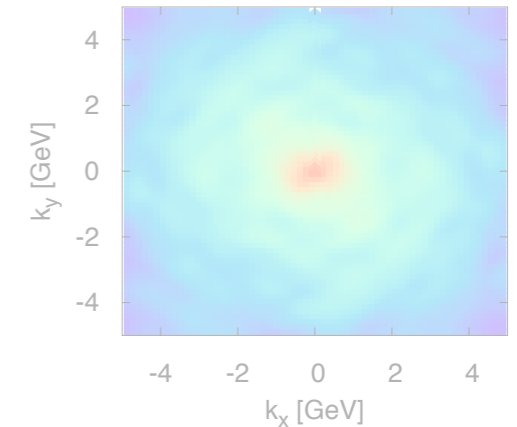


Position space correlations

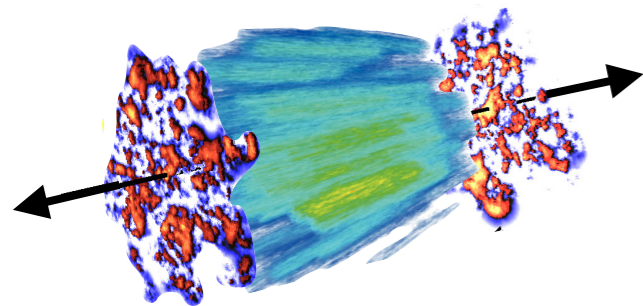
n-gluon distribution

$$\frac{dN_g}{dy} = \frac{2}{N^2} \int \frac{d^2 k_T}{\tilde{k}_T} \left[\frac{g^2}{\tau} \text{tr} (E_i(\mathbf{k}_\perp) E_i(-\mathbf{k}_\perp)) + \tau \text{tr} (\pi(\mathbf{k}_\perp) \pi(-\mathbf{k}_\perp)) \right]$$

Input to PYTHIA, p+p collisions



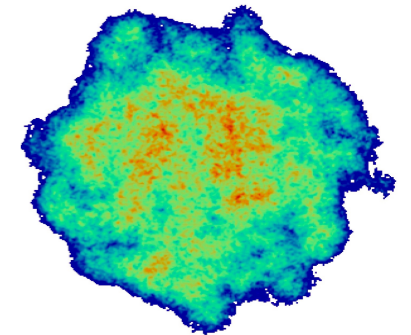
Light-cone gauge-fields



Position space correlations : Stress-Energy Tensor

$$T^{\mu\nu} = -g^{\gamma\delta} F_\gamma^\mu F_\delta^\nu + \frac{1}{4} g^{\mu\nu} F_\delta^\gamma F_\gamma^\delta$$

Input to hydro, transport, p+A, A+A collisions

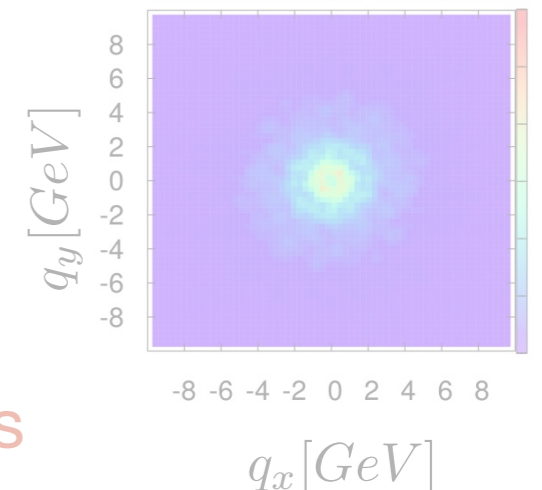


$$U(\mathbf{x}_T) = \mathbb{P} \exp \left\{ ig \int dx^- A^+(x^-, \mathbf{x}_T) \right\}$$

Dipole-gluon & WWs TMDs

$$xG_{\text{WW}}^{ij}(x, \vec{k}) = \frac{8\pi}{L^2} \int \frac{d^2 \mathbf{x}_T}{(2\pi)^2} \frac{d^2 \mathbf{y}_T}{(2\pi)^2} e^{-i\mathbf{k}_T \cdot (\mathbf{x}_T - \mathbf{y}_T)} \times \langle A_a^i(\mathbf{x}_T) A_a^j(\mathbf{y}_T) \rangle$$

Input for EIC observables e+p/A collisions

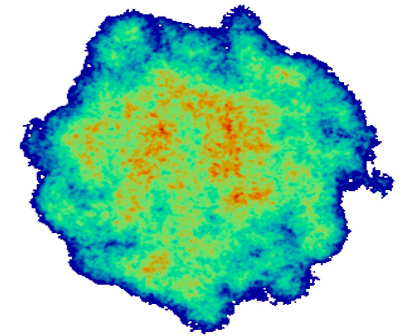


Success of small-x phenomenology in p/A+A

Position space correlations : Stress-Energy Tensor

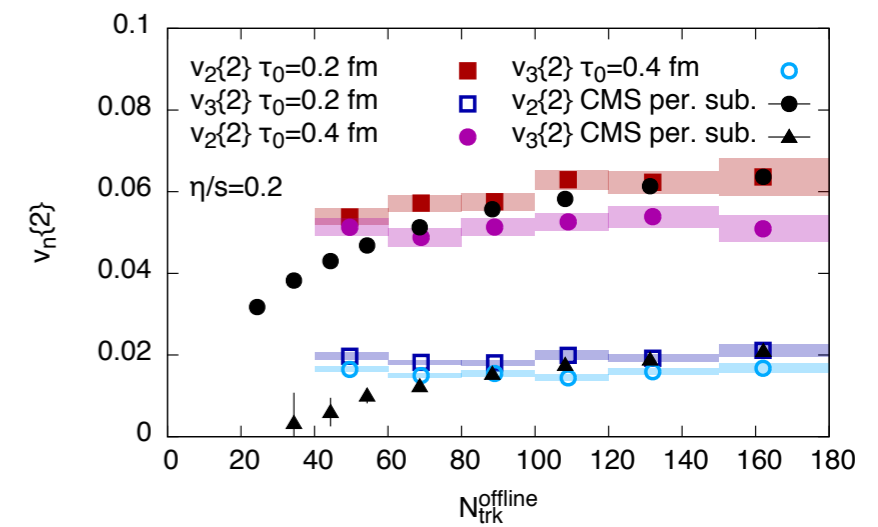
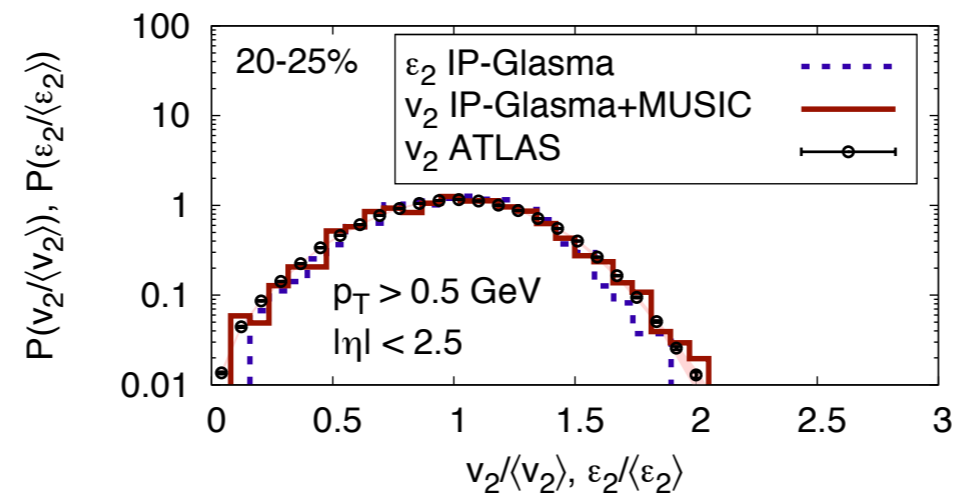
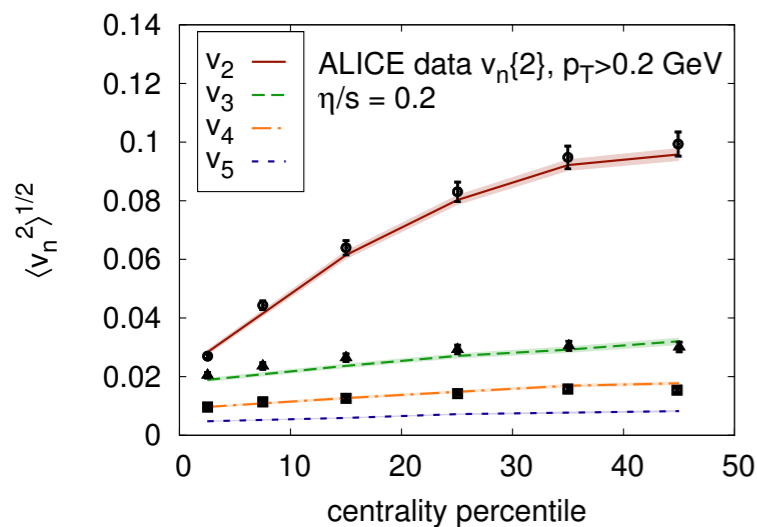
$$T^{\mu\nu} = -g^{\gamma\delta} F_{\gamma}^{\mu} F_{\delta}^{\nu} + \frac{1}{4} g^{\mu\nu} F_{\delta}^{\gamma} F_{\gamma}^{\delta}$$

Input to hydro, transport,
p+A, A+A collisions



Gale, Jeon, Schenke, PT, Venugopalan 1209.6330

Mantysaari, Schenke, Shen, PT 1705.03177

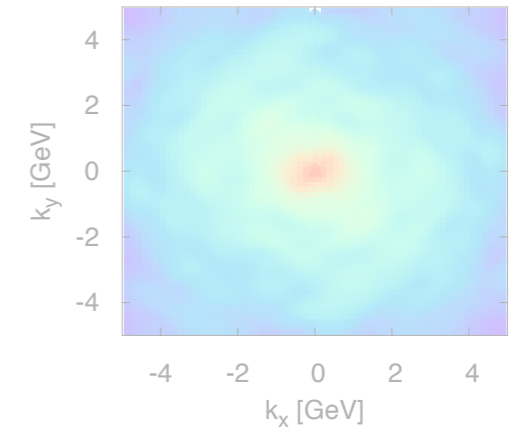


How about EIC observables ?

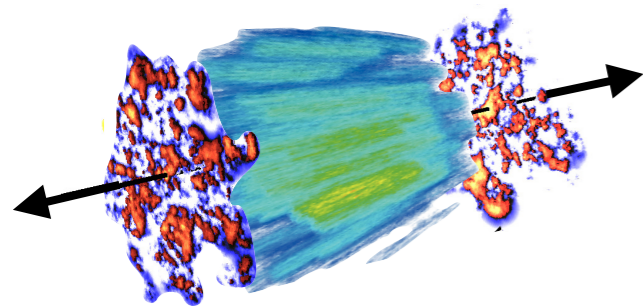
n-gluon distribution

$$\frac{dN_g}{dy} = \frac{2}{N^2} \int \frac{d^2 k_T}{\tilde{k}_T} \left[\frac{g^2}{\tau} \text{tr} (E_i(\mathbf{k}_\perp) E_i(-\mathbf{k}_\perp)) + \tau \text{tr} (\pi(\mathbf{k}_\perp) \pi(-\mathbf{k}_\perp)) \right]$$

Input to PYTHIA, p+p collisions



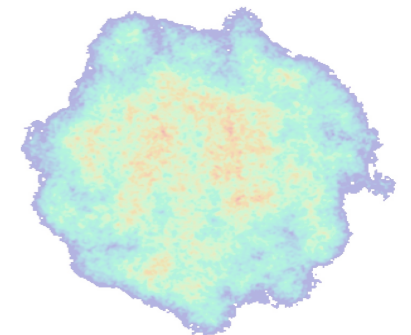
Light-cone gauge-fields



Stress-Energy Tensor

$$T^{\mu\nu} = -g^{\gamma\delta} F_\gamma^\mu F_\delta^\nu + \frac{1}{4} g^{\mu\nu} F_\delta^\gamma F_\gamma^\delta$$

Input to hydro, transport, p+A, A+A collisions

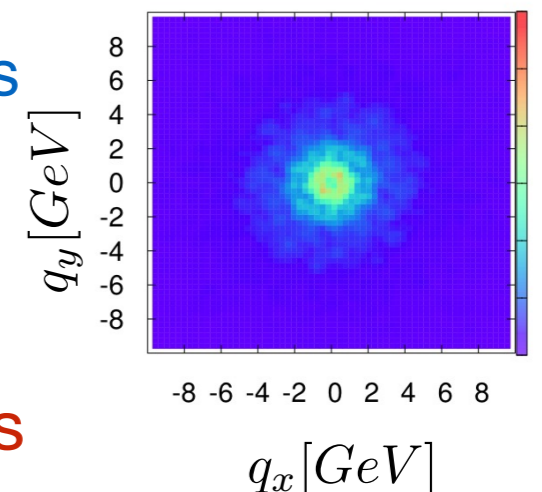


$$U(\mathbf{x}_T) = \mathbb{P} \exp \left\{ ig \int dx^- A^+(x^-, \mathbf{x}_T) \right\}$$

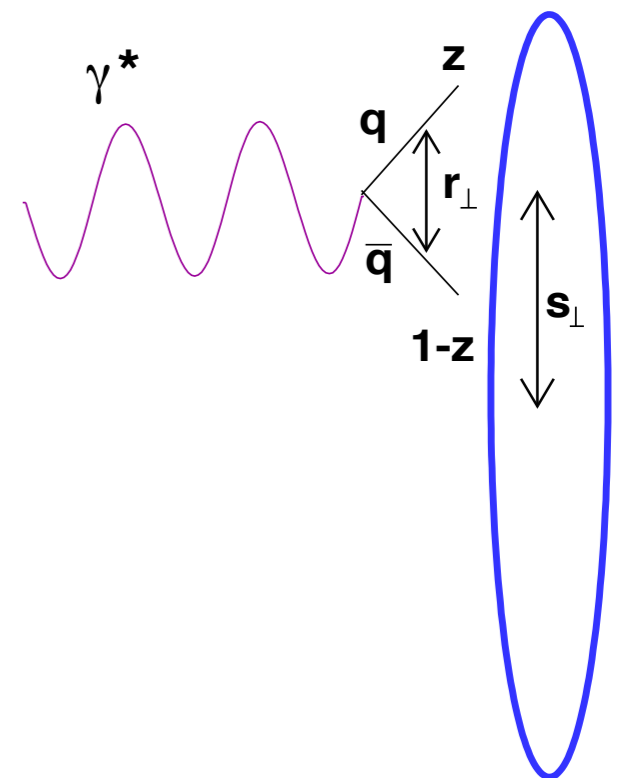
Wave functions: Dipole-gluon & WWs TMDs

$$xG_{\text{WW}}^{ij}(x, \vec{k}) = \frac{8\pi}{L^2} \int \frac{d^2 \mathbf{x}_T}{(2\pi)^2} \frac{d^2 \mathbf{y}_T}{(2\pi)^2} e^{-i\mathbf{k}_T \cdot (\mathbf{x}_T - \mathbf{y}_T)} \times \langle A_a^i(\mathbf{x}_T) A_a^j(\mathbf{y}_T) \rangle$$

Input for EIC observables e+p/A collisions



Towards phenomenology of EIC



Steps towards EIC observables

General ingredients : TMDs that appear in different processes

Dipole gluon distribution (DP) : ($G^{(2)}$) + linearly polarized partner ($h^{(2)}$).

Weizsacker-Williams (WW) : gluon distribution ($G^{(1)}$) + linearly polarized partner ($h^{(1)}$).

Table: D. Boer 1611.06089, V. Skokov

	DIS	DY	SIDIS	$pA \rightarrow \gamma \text{jet} X$	$ep \rightarrow e' Q \bar{Q} X$ $ep \rightarrow e' j_1 j_2 X$	$pp \rightarrow \eta_{c,b} X$ $pp \rightarrow H X$	$pp \rightarrow J/\psi \gamma X$ $pp \rightarrow \Upsilon \gamma X$	$pA \rightarrow j_1 j_2 X$
$G^{(1)}$ (WW)	×	×	×	×	√	√	√	√
$G^{(2)}$ (DP)	√	√	√	√	×	×	×	√

	$pp \rightarrow \gamma \gamma X$	$pA \rightarrow \gamma^* \text{jet} X$	$ep \rightarrow e' Q \bar{Q} X$ $ep \rightarrow e' j_1 j_2 X$	$pp \rightarrow \eta_{c,b} X$ $pp \rightarrow H X$	$pp \rightarrow J/\psi \gamma X$ $pp \rightarrow \Upsilon \gamma X$
$h^{(1)}$ (WW)	√	×	√	√	√
$h^{(2)}$ (DP)	×	√	×	×	×

Mantysaari et al 1712.02508, Dumitru et al Phys. Rev. D 94, 014030 (2016), Dumitru et al Phys. Rev. Lett. 115 (2015) 25, 252301, Zheng et al Phys. Rev. D 89, 7, 074037 (2014), Toll et al, Phys. Rev. C 87, 024913 (2013), F. Dominguez et al Phys.Rev. D85 (2012) 045003, Metz et al Phys.Rev. D84 (2011) 051503, Dominguez et al Phys.Rev. D83 (2011) 105005, Boer et al Phys.Rev. D80 (2009) 094017, Mulders et al Phys.Rev. D63 (2001) 094021

Inclusive dijets at the EIC

Dumitru et al Phys. Rev. D 94, 014030 (2016),
Dumitru et al Phys. Rev. Lett. 115 (2015) 25, 252301

$$e A \rightarrow e' Q \bar{Q} X$$

$$e A \rightarrow e' j_1 j_2 X$$

Azimuthal anisotropy in DIS dijet production
are long range & probe WW TMDs in nuclei

$$E_1 E_2 \frac{d\sigma^{\gamma_L^* A \rightarrow q \bar{q} X}}{d^3 k_1 d^3 k_2 d^2 b} = \alpha_{em} e_q^2 \alpha_s \delta(x_{\gamma^*} - 1) z^2 (1-z)^2 \frac{8\epsilon_f^2 P_\perp^2}{(P_\perp^2 + \epsilon_f^2)^4}$$

$$\times \left[xG^{(1)}(x, q_\perp) + \cos(2\phi) xh_\perp^{(1)}(x, q_\perp) \right]$$

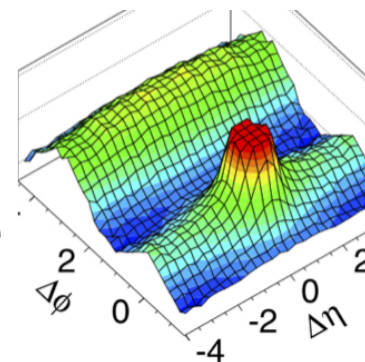
Weizsacker-Williams (WW) : gluon distribution ($G^{(1)}$) + linearly polarized partner ($h^{(1)}$)

$$\vec{P}_\perp = (1-z)\vec{k}_1 - z\vec{k}_2, \quad \vec{q}_\perp = \vec{k}_1 + \vec{k}_2$$

Rapidity imbalance $\xi = \log \frac{1-z}{z}$

Relative azimuth $\phi = (\vec{P}_\perp \cdot \vec{q}_\perp) / (|\vec{P}_\perp| |\vec{q}_\perp|)$

Analogy to $\Delta\eta$ - $\Delta\phi$ ridge

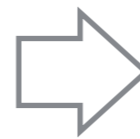
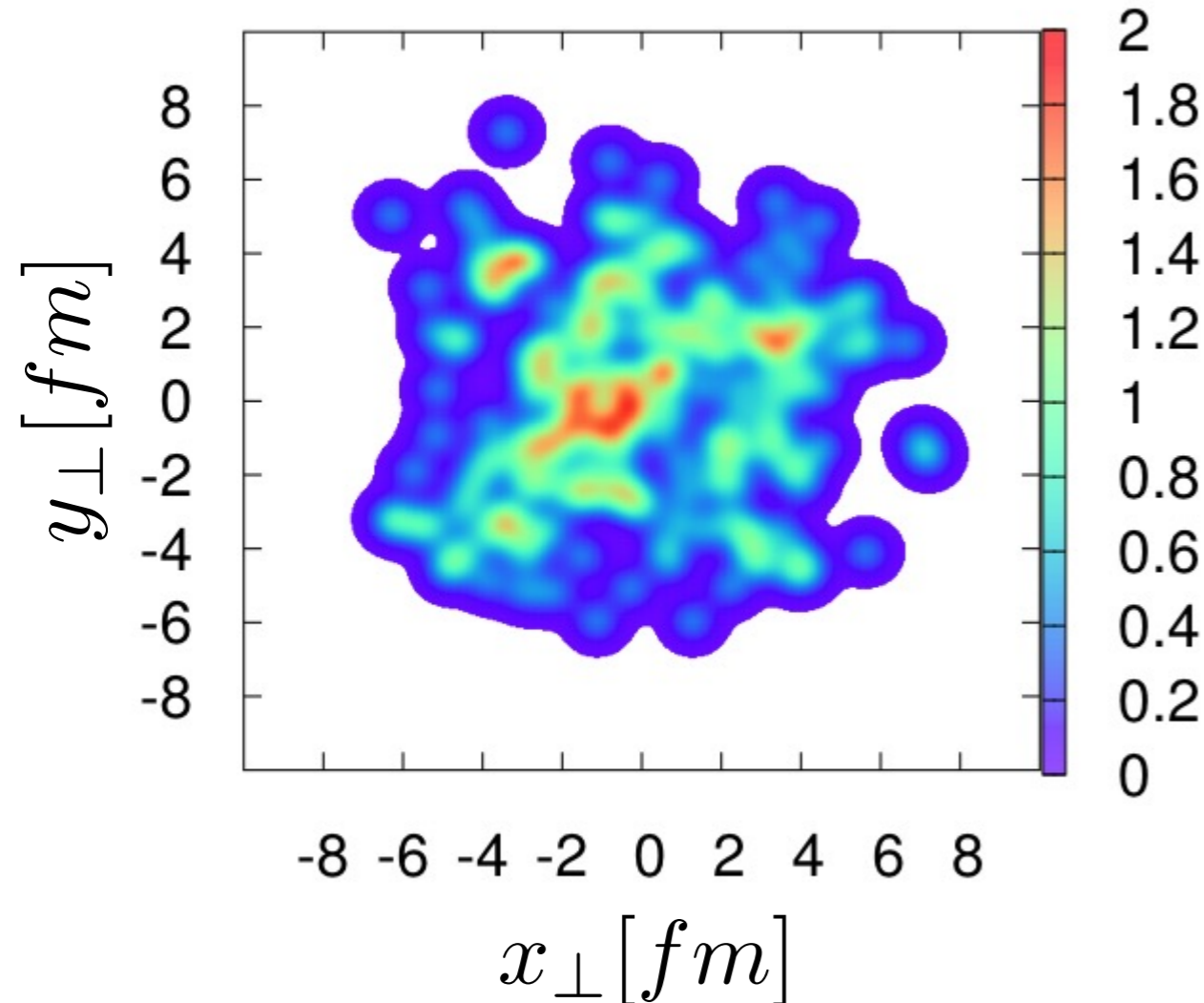


Step1: TMDs from the IP-Sat model for nuclei

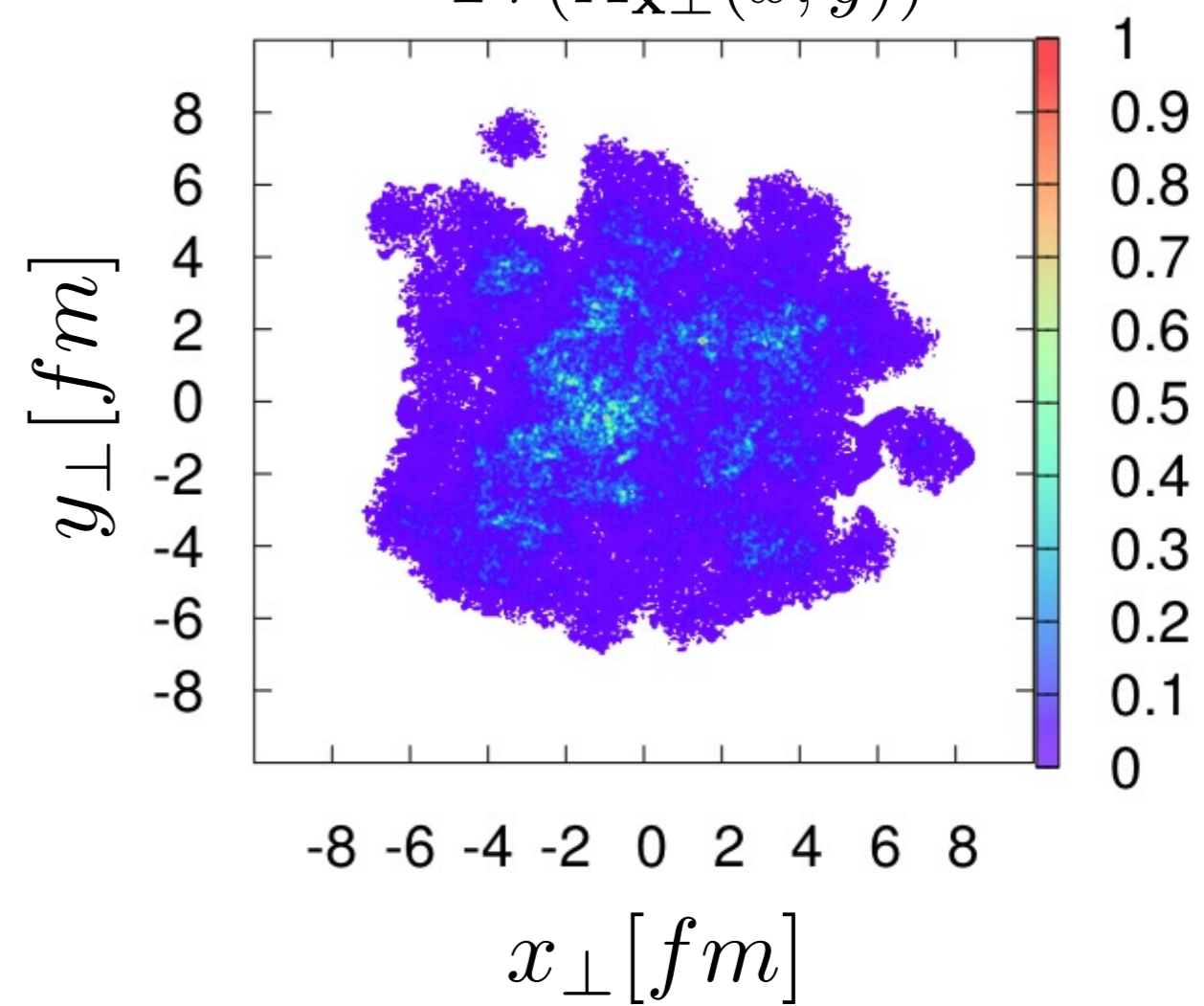
$$U(\mathbf{x}_T) = \mathbb{P} \exp \left\{ ig \int dx^- A^+(x^-, \mathbf{x}_T) \right\}$$

$$A^i(\mathbf{x}_T) = \frac{1}{ig} U^\dagger(\mathbf{x}_T) \partial_i U(\mathbf{x}_T)$$

$$\langle \rho(\mathbf{x}_{1\perp}) \rho(\mathbf{x}_{2\perp}) \rangle$$



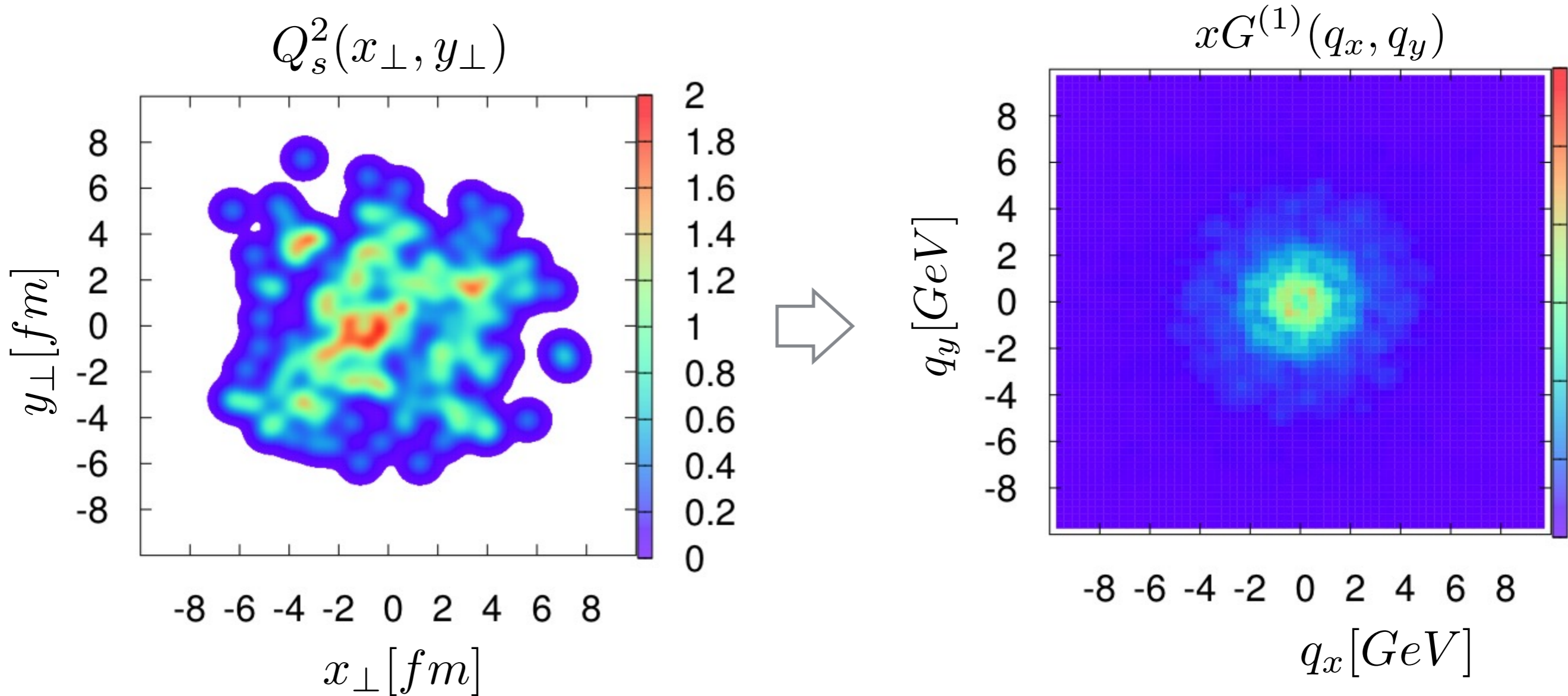
$$Tr(A_{\mathbf{x}_\perp}(x, y))$$



We apply the approach similar to small-x phenomenology in p+A, A+A

Weizsacker-Williams gluon distributions

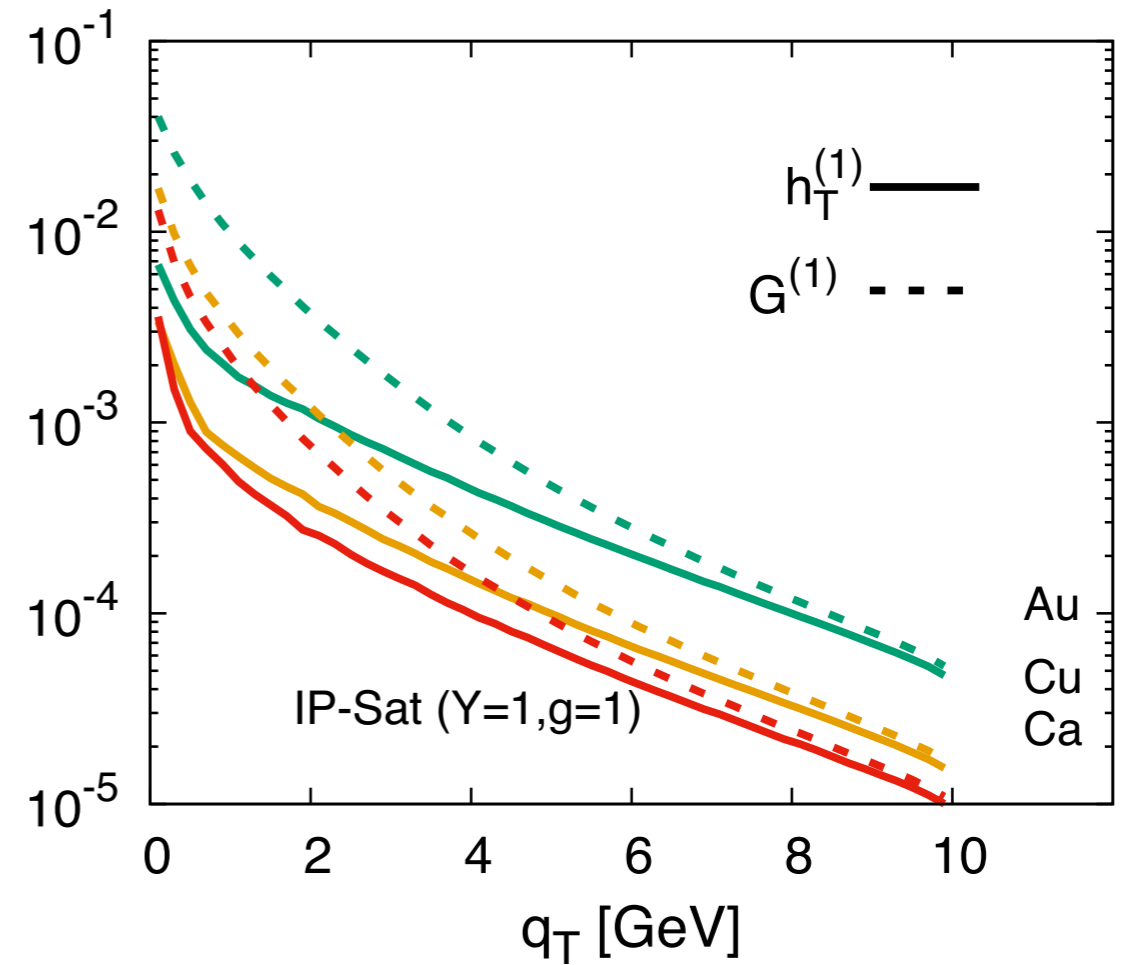
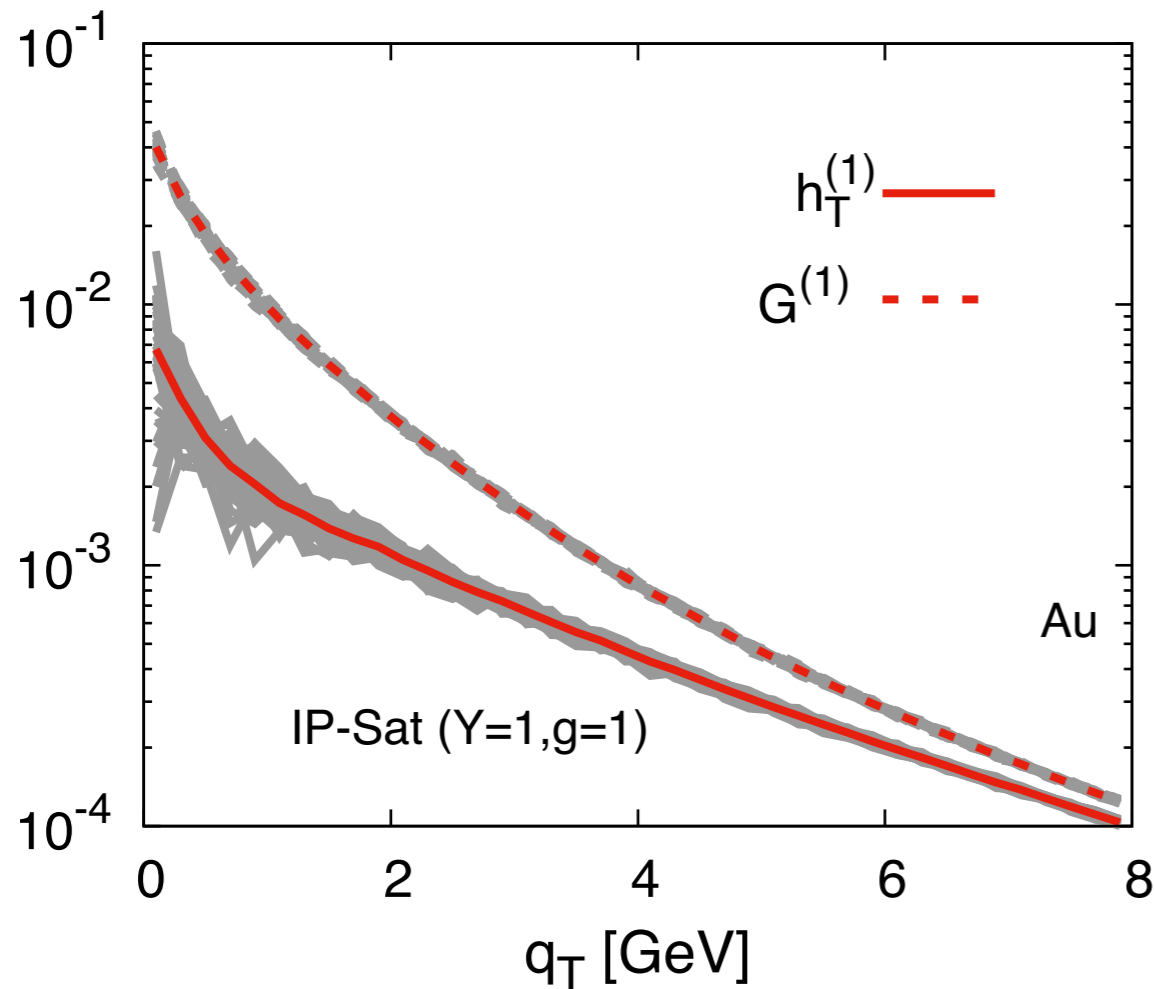
$$xG_{\text{WW}}^{ij}(x, \vec{k}) = \frac{8\pi}{L^2} \int \frac{d^2\mathbf{x}_T}{(2\pi)^2} \frac{d^2\mathbf{y}_T}{(2\pi)^2} e^{-i\mathbf{k}_T \cdot (\mathbf{x}_T - \mathbf{y}_T)} \langle A_a^i(\mathbf{x}_T) A_a^j(\mathbf{y}_T) \rangle$$



$$xG_{\text{WW}}^{ij} = \frac{1}{2} \delta^{ij} xG^{(1)} - \frac{1}{2} \left(\delta^{ij} - 2 \frac{k^i k^j}{k^2} \right) xh_\perp^{(1)}$$

Weizsacker-Williams gluon distributions

$$xG_{\text{WW}}^{ij} = \frac{1}{2} \delta^{ij} xG^{(1)} - \frac{1}{2} \left(\delta^{ij} - 2 \frac{k^i k^j}{k^2} \right) xh_{\perp}^{(1)}$$



TMDs for different nuclei at fixed rapidity,
JIMWLK evolution left for future work

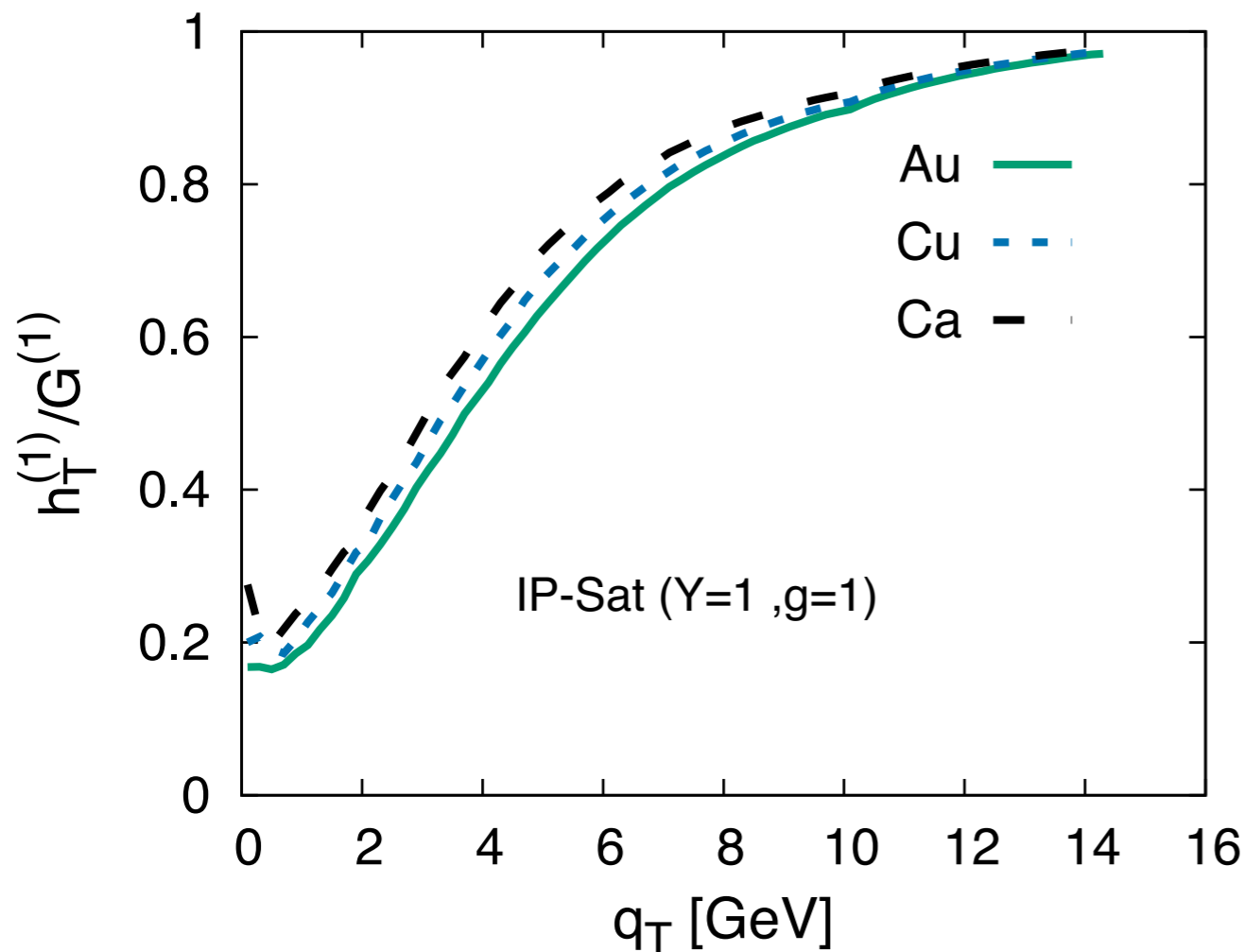
Step2: WW gluon distributions & q-qbar jets in DIS

$$xG_{\text{WW}}^{ij} = \frac{1}{2} \delta^{ij} xG^{(1)} - \frac{1}{2} \left(\delta^{ij} - 2 \frac{k^i k^j}{k^2} \right) xh_{\perp}^{(1)}$$

Dumitru, Lappi, Skokov Phys.Rev.Lett. 115 (2015) 25, 252301

$$E_1 E_2 \frac{d\sigma^{\gamma_L^* A \rightarrow q\bar{q}X}}{d^3k_1 d^3k_2 d^2b} = \alpha_{em} e_q^2 \alpha_s \delta(x_{\gamma^*} - 1) z^2 (1-z)^2 \frac{8\epsilon_f^2 P_{\perp}^2}{(P_{\perp}^2 + \epsilon_f^2)^4}$$

$$\times \left[xG^{(1)}(x, q_{\perp}) + \cos(2\phi) xh_{\perp}^{(1)}(x, q_{\perp}) \right]$$



Quark-antiquark jet correlation
azimuthal anisotropy in DIS

Large long-range azimuthal
correlations in DIS dijet
production predicted which
probes WW TMDs in nuclei

Another connection : chiral magnetic effect



Contact: Karen McNulty Walsh, (631) 344-8350, or Peter Genzer, (631) 344-3174

share:

Relativistic Heavy Ion Collider Begins 18th Year of Experiments

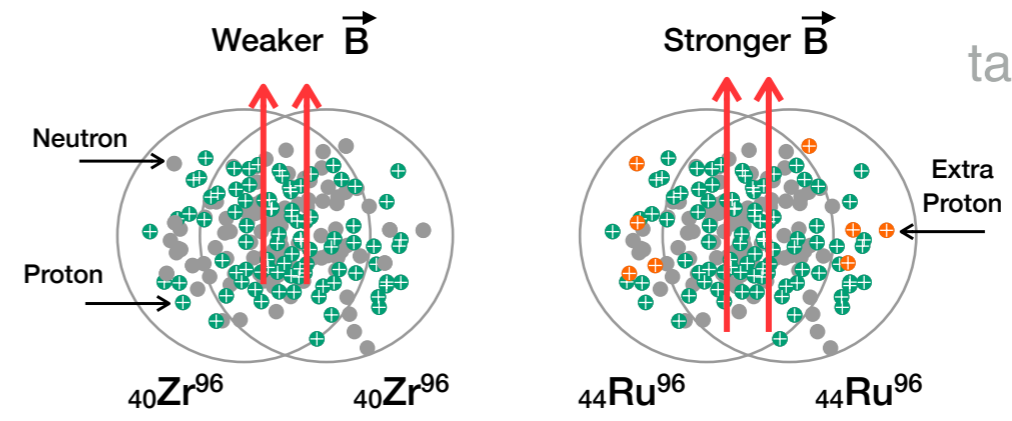
First smashups with 'isobar' ions and low-energy gold-gold collisions will test earlier hints of exciting discoveries as accelerator physicists tune up technologies to enable future science

March 21, 2018



QCD anomaly driven chirality imbalance leads to electric current along B-field

RHIC is doing Isobar collisions to search for the Chiral Magnetic Effect



talk by Wei Li

Lappi, Schlichting
1708.08625

Signals of CME → Axial charge density correlator :

$$\propto (G_{A1}^{(1)}(x, y))^2 (G_{A2}^{(1)}(x, y))^2 - (h_{\perp A1}^{(1)}(x, y))^2 (h_{\perp A2}^{(1)}(x, y))^2$$

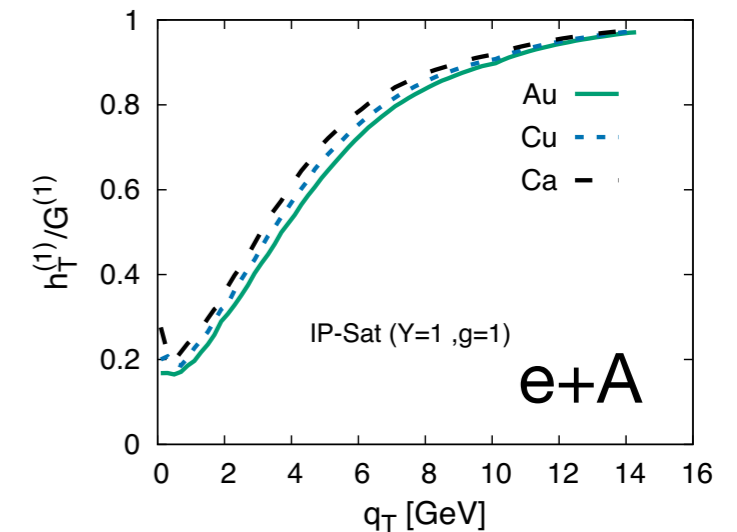
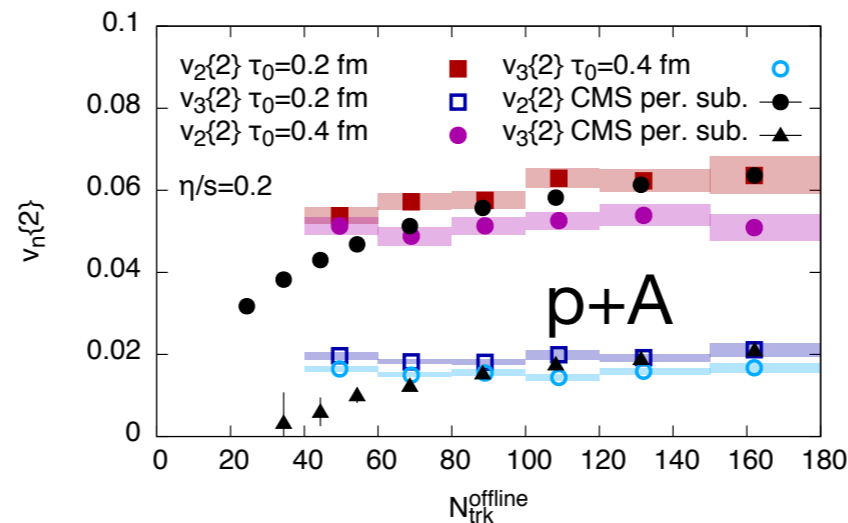
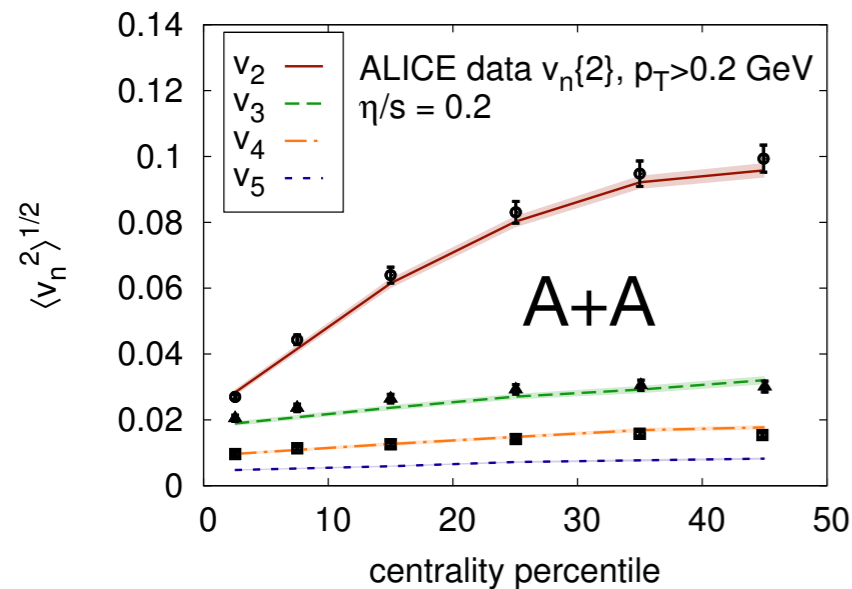
Experimental observable : charged dependent azimuthal correlations

This also probes TMDs (will enable us to make better predictions for EIC)

Summary

Constraints from DIS + CGC framework have revolutionized p+p, p+A, A+A phenomenology over past years at RHIC & LHC energies

Long range azimuthal anisotropy is the key observable across different systems



We can follow the same path of EIC :

- The fundamental ingredients are TMDs for EIC observables
- TMDs can be estimated consistently in the small-x approach
- Large long-range $\cos(2\phi)$ anisotropy in DIS dijets is predicated to probe TMDs

Lessons from RHIC/LHC will be helpful to build Monte-Carlo generators for EIC

Thank you